Chapter 6

Basic Aspects of Gas Turbine Heat Transfer

Shailendra Naik

Additional information is available at the end of the chapter

http://dx.doi.org/10.5772/67323

Abstract

The use of gas turbines for power generation and electricity production in both single cycle and combined cycle plant operation is extensive and will continue to globally grow into the future. Due to its high power density and ability to convert gaseous and liquid fuel into mechanical work with very high thermodynamic efficiencies, significant efforts continue today to further increase both the power output and thermodynamic efficiencies of the gas turbine. In particular, the aerothermal design of gas turbine components has progressed at a rapid pace in the last decade with all gas turbine manufacturers, in order to achieve higher thermodynamic efficiencies. This has been achieved by using higher turbine inlet temperatures and pressures, advanced turbine aerodynamics and efficient cooling systems of turbine airofoils, and advanced high temperature alloys, metallic coatings, and ceramic thermal barrier coatings. In this chapter, issues related to the thermal design of gas turbine blades are highlighted and several heat transfer technologies are examined, such as convective cooling, impingement cooling, film cooling, and application of thermal barrier coatings. Typical methods for validating the thermal designs of gas turbine airofoils are also outlined.

Keywords: gas turbines, airofoils, efficiency, heat transfer, aerodynamics, film cooling, convective cooling, impingement, turbulator, pins, thermal barrier coating, compressible flows

1. Introduction

The aerothermal design of advanced gas turbines has progressed significantly in the last decade, primarily due to the requirement of increased turbine efficiencies and power. Performance increases are driven not only for reducing the consumption of fuel and the subsequent cost benefits, but also to reduce the emissions of CO_2, which is a primary component for the increased global warming. Over the last decade, major gas turbine performance enhancements have been achieved by the use of higher turbine inlet temperatures and pressures, design of advanced turbine aerodynamics, through reductions in turbine cooling and leakage

air, and via the introduction of new high temperature alloys, metallic antioxidation coatings, and thermal barrier coatings. In today's energy market, there is wide range of gas turbines ranging from 1 to 500 MW and can operate with low and high calorific fuels. **Figure 1** shows the GT26 heavy duty gas turbine [1, 2].

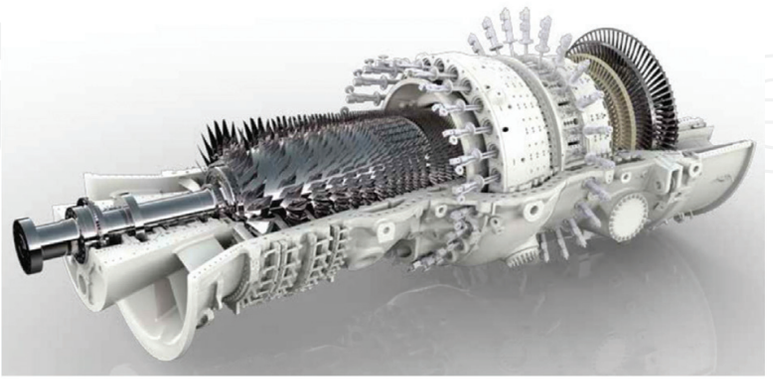

Figure 1. Heavy duty gas turbine, GT26.

The operation of a gas turbine, which essentially consists of four major components; compressor, combustor, turbine, and the exhaust diffuser, is governed by the Brayton thermodynamic cycle. For simple power generation applications, a generator is normally coupled to the gas turbine, whereby the mechanical work generated by the turbine is converted to useful electrical energy. In today's energy market, most gas turbine-based power plants are operated in combined cycle operation mode. **Figure 2** shows a typical component layout of a combined cycle plant, whereby the gas turbine plant is coupled to a steam turbine plant via the heat recovery steam generator. Thermodynamically, the gas turbine operates in a Brayton cycle, whereas the steam turbine operates in a Rankine cycle. Due to this combination, **Figure 2** highlights that combined cycle efficiencies are significantly higher than that of a gas turbine in simple operation. There are many variations of the gas turbine combined cycle plant and the interdependency of the component efficiencies and plant operating conditions. An extensive overview of industrial gas turbine combined cycle plant is given in Ref. [1].

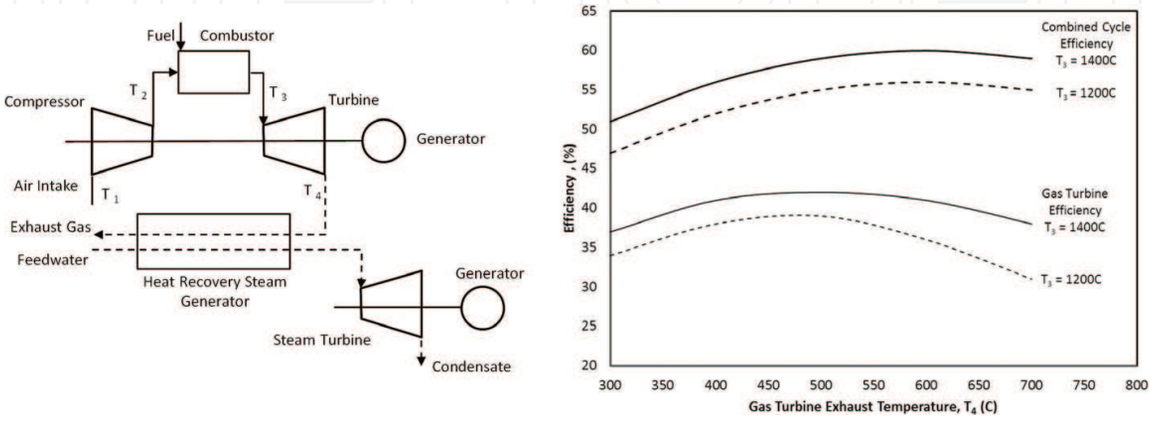

Figure 2. Basic combined cycle plant arrangement, adapted from Ref. [1].

http://dx.doi.org/10.5772/67323

The historical progress in increased combined cycle plant efficiencies was recently reviewed in Ref. [3] and is highlighted in **Figure 3**, which predicts a continuous growth in cycle efficiencies approaching 65% over the next decades. **Figure 3** also shows that a major part of the current growth in combined cycle efficiencies is attributed to improvements in gas turbine thermodynamic efficiencies, particularly with the H and J class gas turbines. A key driver for the latter has been the increased turbine inlet temperatures, and as shown in **Figure 4**, this has also resulted in the development of high-grade alloy, coatings, and very efficient airofoil cooling designs which can maintain the blade metal temperatures and structural integrity for long continuous operating periods. In this chapter, issues related to the thermal design of gas turbine blades are examined and the various cooling technologies are outlined. In addition, typical methods for validating the thermal designs of gas turbine airofoils are also outlined.

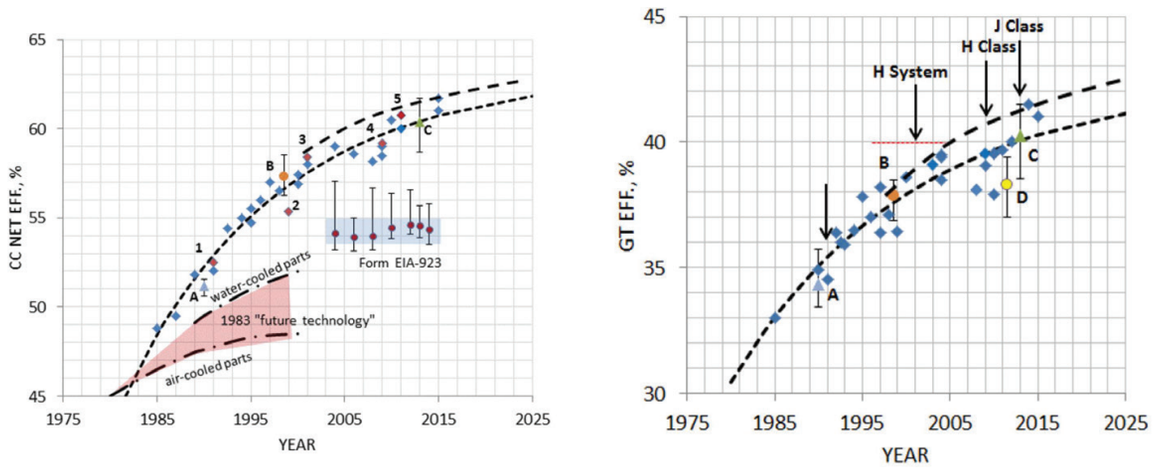

Figure 3. Performance evolution of combined cycle and single cycle gas turbine [3].

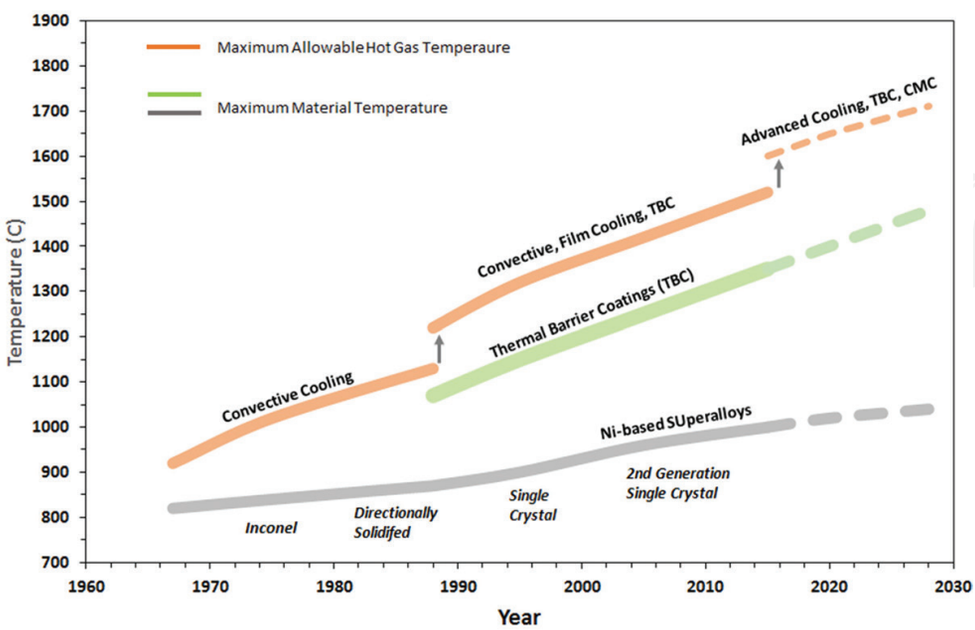

Figure 4. Evolution of gas turbine hot gas temperatures, materials, and cooling technology, adapted from Ref. [7].

2. Design consideration of cooled turbine blades

In the design of air cooled gas turbine blades, there are several different factors related to the integration of a turbine blade thermal design into the overall gas turbine. Some of the key factors which influence the overall design of the turbine blade include [4–6, 51],

- Overall gas turbine performance (power output and efficiency) and airofoil component lifetime requirements.
- Variation of ambient conditions, start-up load gradients, and shut-down conditions.
- Turbine aerodynamics, external heat loads to airofoils and turbine inlet temperatures.
- Hot gas temperature, pressure, and velocity profiles from the combustor chamber, and the expansion characteristics of the hot gas within the turbine.
- Choice of coolant from the compressor bleeds and the supply conditions over the entire operating envelope of the gas turbine.
- Geometrical clearances and gaps.
- Blade material and its properties at elevated temperatures.
- Manufacturing capability of the blade internal cooling core, machining of film cooling holes, application of thermal barrier coatings, and overall manufacturing costs.
- Maintenance methods and reconditioning of the turbine blades.

In **Figure 5**, some of the above parameters are highlighted, such as the impact of the coolant extracted from the different stages of the compressors. The front stage of the turbine will normally use the coolant extracted with the highest pressures, while the middle and rear turbine stages progressively use coolant extracted with lower pressures and temperatures. For the rear stage airofoils, the cooling systems are normally low pressure drops systems and do not have features such as film cooling and impingement cooling. The front stage airofoils however do have cooling systems with film cooling and impingement, as they are generally fed with the high pressure compressor end air. In addition to the impact of the air flow system, another major interface parameter for designing the airofoil cooling system is the combustor hot gas temperature and its distribution [8]. **Figure 5** shows a schematic of the hot gas distribution at the turbine inlet, which is generally nonuniform, and dependant on the upstream combustor and burner design. As **Figure 5** shows, typically there is a radial distribution of the hot gas temperature, which is commonly referred to as the profile factor or the radial temperature distortion factor (RTDF). In addition to this, there is also a circumferential temperature distribution which is referred to as the pattern factor or the outer temperature distortion factor (OTDF). In the thermal design of gas turbine airofoils, blade tips, and endwalls, these radial and circumferential temperature distributions are always considered in the design process, and are normally based on in-situ engine measurements and high fidelity CFD predictions.

http://dx.doi.org/10.5772/67323

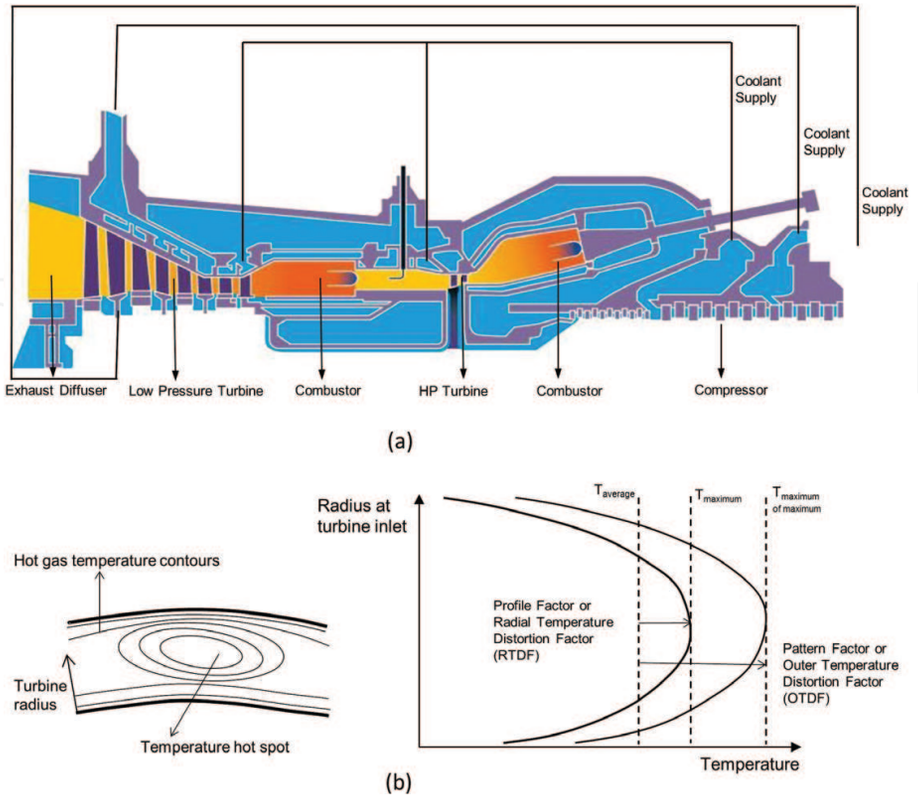

Figure 5. Major design factors influencing the gas turbine overall aerothermal design, (a) coolant supply system, (b) combustor hot gas temperature profiles.

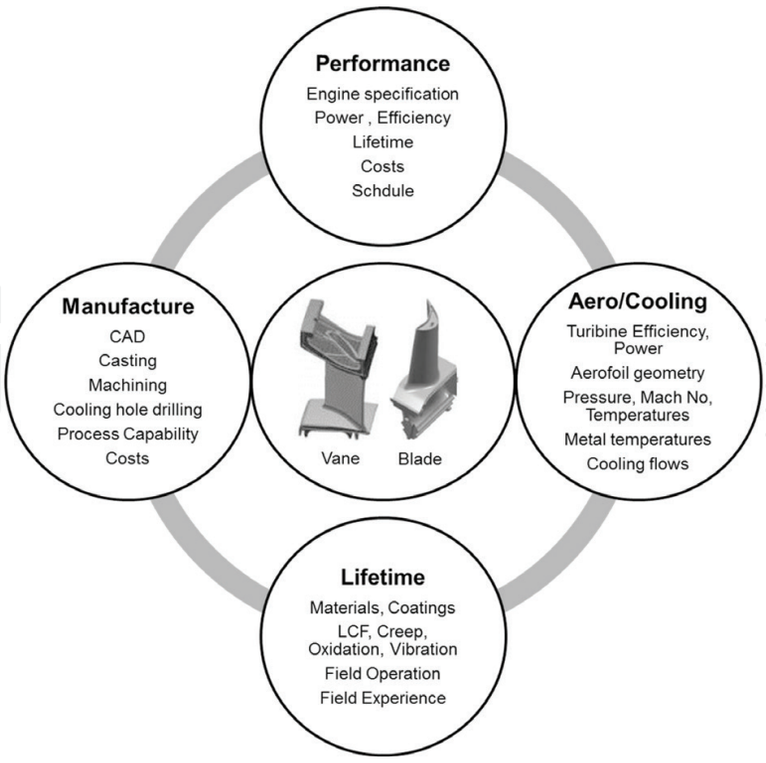

Figure 6. Major design interfaces for overall airofoil designs.

At the airofoil component level design, **Figure 6** shows an overview of several other interface considerations which needs to be accounted for in the overall optimization of the airofoil thermal design. The major design drivers for an optimized airofoil design include engine performance targets, aerothermal targets, component lifetime and mechanical integrity targets, and the manufacturing and cost constraints. Within these global requirements, **Figure 6** also highlights that are also many subtargets, such as manufacturing capability and field experience.

3. Turbine blade thermal analysis

3.1. Global thermal assessments

Due to the large number of operating and geometrical parameters that influence the heat transfer mechanism in gas turbine blades, simplified zero-dimensional relationships and design charts are often utilized. This allows for assessing the impact of various operational and geometrical parameters on a given blade cooling system. For such zero-dimensional analysis, it is important to have the detailed 2D and 3D thermal analysis results of the specific turbine blade or vane, and which has effectively been proven for meeting the design performance and lifetime in field gas turbines. This is commonly referred to as the reference blade from which new designs and concepts can be developed with a sufficient degree of confidence.

The thermal analysis is based on a simplified conjugate heat transfer analysis of flow in a cooling passage of a turbine blade as shown in **Figure 7** and assumes that the airofoil; (a) metal temperature is the average surface temperature at the airofoil midspan, (b) is exposed to the maximum hot gas temperature profile at the blade inlet, and (c) the coolant enters at the blade root and exits at the blade trailing edge. Then by performing a simple energy balance, it can be observed that,

Heat transferred from the hot gas to the airofoil = heat gained by the airofoil = heat gained by the coolant in the airofoil.

$$Q = h_g S_g L \left(T_f - T_m\right) = h_c S_c L \left(T_m - T_c\right) = m_c C_{pc} \left(T_{co} - T_{ci}\right) \tag{1}$$

where Q is the total heat transferred to the airofoil, h_g and h_c are respectively the hot gas and coolant heat transfer coefficients, L is the airofoil height, S_g and S_c are respectively the total airofoil perimeter on the gas and coolant sides, T_f is the average film cooling temperature, T_m is the average airofoil metal temperature, and T_{ci} and T_{co} are the coolant inlet and out temperatures. T_c is the average of the coolant inlet and outlet temperatures. For film-cooled airofoils, a film cooling effectiveness is additionally defined, which essentially modifies the driving hot gas temperature, T_g, with a film temperature, which is defined by;

$$\text{Film Cooling Effectiveness,} \qquad \eta_f = \frac{T_g - T_f}{T_g - T_{co}} \tag{2}$$

After rearranging the above equations, the following relationships can be derived;

$$\text{Cooling Effectiveness,} \qquad \varepsilon = \frac{T_g - T_m}{T_g - T_{ci}} \tag{3}$$

$$\text{Mass flow function,} \qquad m^* = \frac{m_c \; C_{pc}}{h_g \; S_g \; L} \tag{4}$$

http://dx.doi.org/10.5772/67323

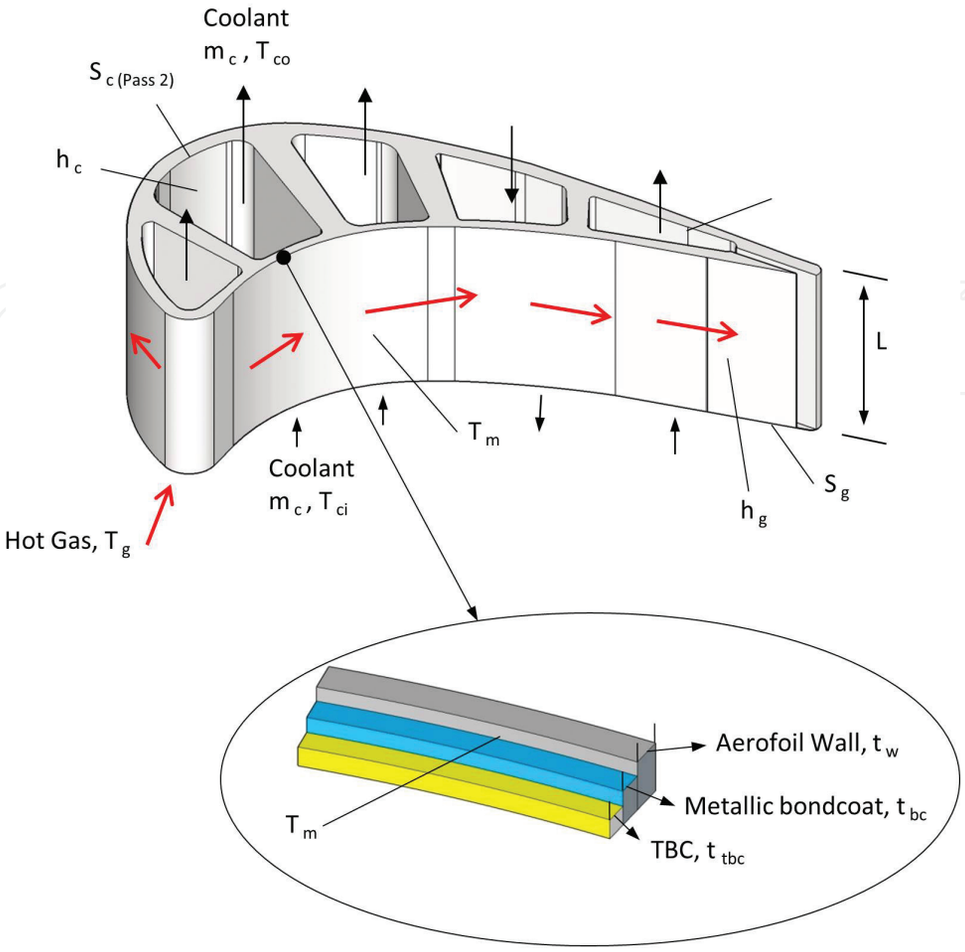

Figure 7. Thermal design parameters of a gas turbine airofoil.

Cooling Efficiency, $$\eta = \frac{T_{co} - T_{ci}}{T_m - T_{ci}} \quad (5)$$

By further combining for the effectiveness, massflow function and efficiency, the following practical engineering formulations can be derived.

Overall effectiveness, $$\varepsilon = \frac{m^* \eta}{1 + m^* \eta} \quad (6)$$

Overall efficiency, $$\eta = 1 - \exp\left[-\frac{A}{m^*}\right] \quad \text{Where } A = \frac{h_c \cdot S_c}{h_g \cdot S_g} \quad (7)$$

To represent thermal barrier coatings (TBC) and the airofoil wall thickness, the hot gas and coolant heat transfer coefficients in the above equations are replaced by effective heat transfer coefficients, i.e.,

$$h_{g,eff} = \frac{h_g}{1 + B\,i_{tbc}} \quad (8), \text{ where the TBC Biot number, } B\,i_{tbc} = \frac{h_g\, t_{tbc}}{k_{tbc}}$$

$$h_{c,eff} = \frac{h_c}{1 + B\,i_w} \quad (9), \text{ where wall Biot number, } B\,i_w = \frac{h_c\, t_w}{k_w}.$$

Where, t_{tbc} and k_{tbc} are the thermal barrier coating thickness and thermal conductivity, respectively. Similarly, t_w and k_w are the metal wall thickness and thermal conductivity. From the above relationship, it can be observed that for the extreme cases, when $\varepsilon = 0$, $T_m = T_{hg}$, the

airofoil metal temperature equal the gas temperature, and when $\varepsilon = 1$, $T_m = T_c$ and the airofoil metal temperature equals the coolant temperature. For most gas turbine blades ranging from the rear to the front turbine stages, the effectiveness values are respectively in the range of 0.1–0.7.

Figure 8 shows the relationship between the cooling effectiveness, mass flow function and the cooling efficiency, which is shown in an alternative form to that normally highlighted in Refs. [4–6]. Here, the cooling efficiency and the massflow function parameters are plotted on the horizontal and vertical axis respectively, which makes it easier to compare the cooling efficiencies of different turbines. From **Figure 8**, it is clear the front stages of the gas turbine, which are exposed to the highest hot gas temperatures, will generally have the highest cooling effectiveness and efficiency levels as their cooling designs will include film cooling, thermal barrier coatings, impingement cooling, turbulator convective cooling, and advanced alloys. The rear stages which are generally exposed to the lowest hot gas temperatures are generally convectively cooled, consume the least amount of cooling air, and are represented by the lowest effectiveness and efficiency values.

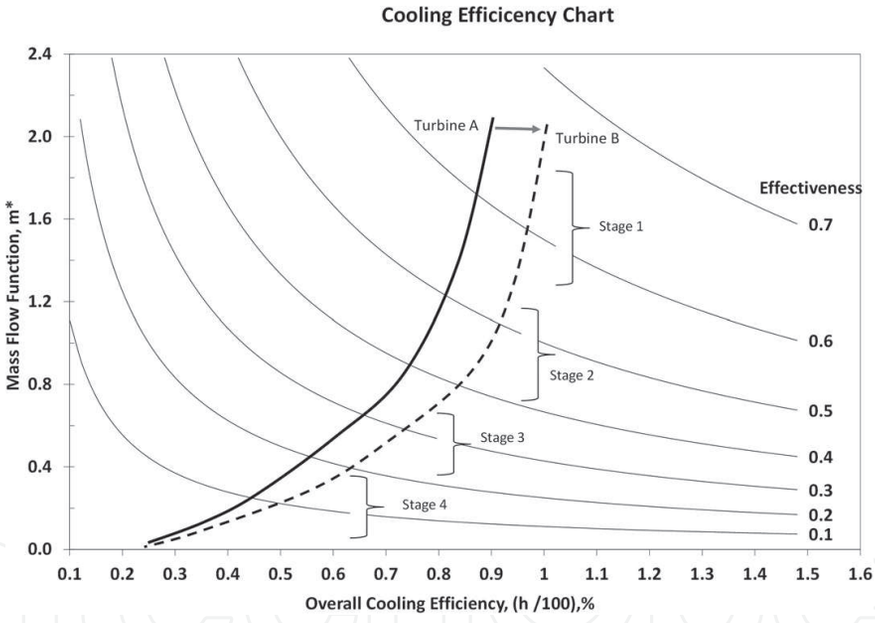

Figure 8. Heat transfer performance chart for gas turbine blades.

3.2. Detailed aerothermal designs

During the detailed design phases, the design of cooled turbine airofoils is normally done using design systems which incorporate the effect of all three-dimensional geometrical and aerothermal effects. There is extensive use of computational fluid dynamics, as part of the overall turbine design process and the thermal analyses are based on conjugate heat transfer-based model. **Figure 9(a)** shows a typical example of a gas turbine blade conjugate heat transfer model [9], where both the internal coolant flows in the internal cooling passages and the external heat

http://dx.doi.org/10.5772/67323

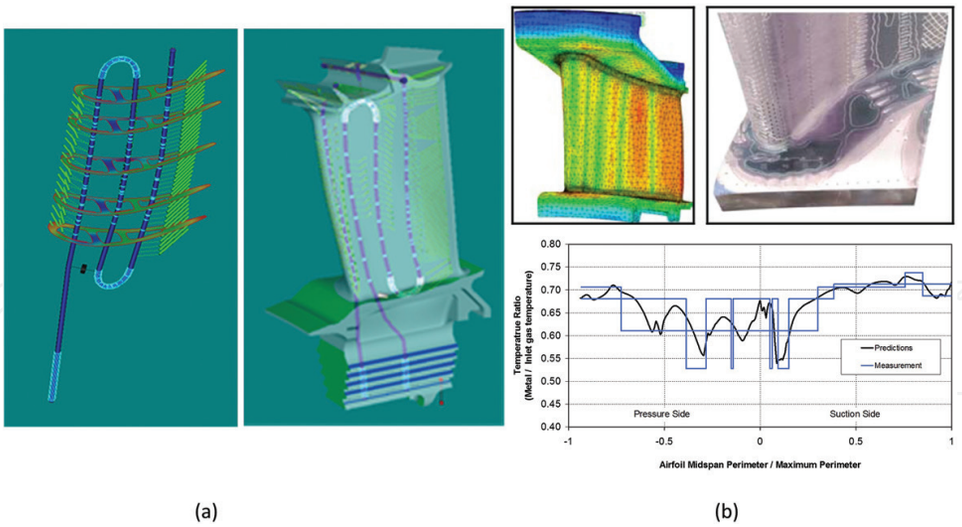

Figure 9. Detailed airofoil aerothermal design using (a) conjugate thermal modelling [9], and (b) 3D thermal modelling and comparisons with measured engine data [2, 10].

loads on the airofoil hot gas surfaces are directly simulated. **Figure 9(b)** shows a typical example of the predicted metal temperature on a turbine vane based on a conjugate heat transfer model and compared to measured metal temperatures from a test engine [2, 10].

4. External heat transfer of cooled turbine airofoils

The aerodynamics of the gas path flows through the static turbine vanes and rotating blades consist of a range of flow phenomena and flow structures such as accelerating sonic and transonic flows, unsteady flows, separated flows, secondary flows, overtip leakage flows, and interacting flows between the main gas path flows and coolant and leakage flows. To enhance the turbine aerodynamic efficiency and manage the external heat loads, significant research efforts have been made over the past decade to minimize the energy losses which are associated with the latter flow phenomenon. Similarly, there has been a significant research effort [4–6, 11, 12], in understanding and minimizing the external heat transfer on the turbine airofoils and endwalls, which is essentially defined by the gas path aerodynamics, thermodynamics, turbine geometrical annulus, and the geometrical profiles of the airofoils.

4.1. Airofoil external heat loads

The aerodynamic development of the boundary layer on the turbine static and rotating airofoils is highly nonuniform, and it largely determines the absolute levels of the external heat transfer coefficient to which it will be exposed. Other factors that significantly influence the airofoil heat transfer include the mainstream turbulence, profile curvature, streamwise pressure gradients, surface roughness, upstream wakes, and film cooling. **Figure 10** shows the Mach number measured on a turbine vane and blade [13], and highlights; (a) the strong Mach

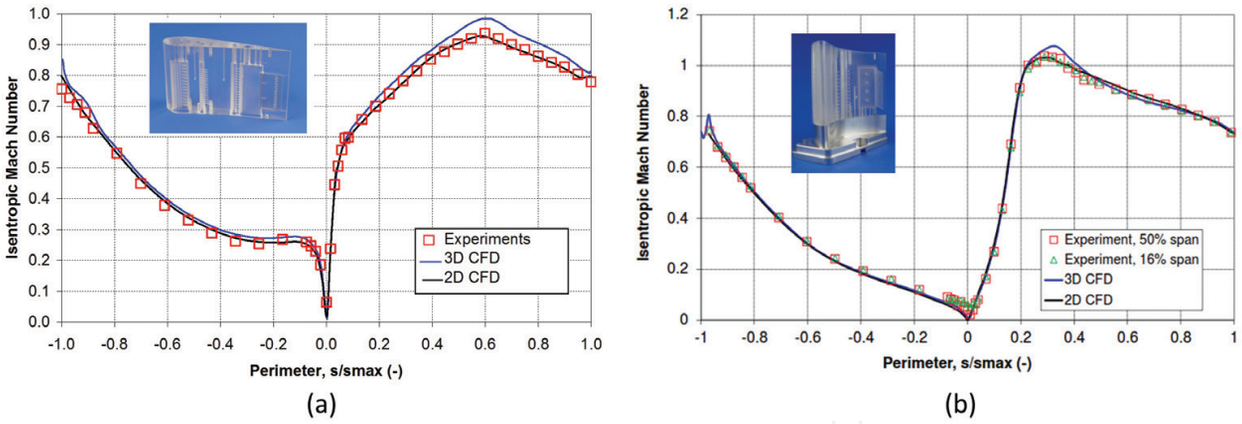

Figure 10. Aerodynamic measurements and predictions on a 1st stage (a) vane and (b) blade [12].

number variations near the leading edge stagnation point, (b) accelerating flow on the pressure and suction sides immediately downstream of the leading edge, (c) region of transitional boundary layer, (d) regions of accelerating turbulent flows on the pressure side, and (e) regions of peak Mach numbers on the suction side followed by decelerating flows towards the trailing edge. It is this variation in the profile Mach number which largely determines the vane and blade external heat transfer coefficients.

The detailed distribution of the heat transfer coefficients on the turbine vane and blade of a high pressure turbine was measured by Tallman et al. [12] for a range of operating conditions. **Figure 11** shows the distribution of the measured and predicted Stanton numbers, (St = Nu/Re.Pr) at 50% airofoil span and at Re/L = 3.1 e6, and clearly highlights the differences in the heat transfer distribution between the vane and the blade. This is largely due to the different profile shapes, leading edge diameters, Mach number distributions, and the overall pressure ratio across the vane and blade. **Figure 11** highlights the heat transfer distribution associated with the various aerodynamic flow regimes on the airofoil. For the vane, the heat transfer coefficient increases from the leading edge to the suction side, reaches a peak value, and then decelerates towards the trailing edge. On the pressure side, it reduces from the leading edge and after transition, continuously accelerates up to the trailing edge. For the blade, the peak heat transfer coefficient value is at the leading edge, which then decreases gradually on the

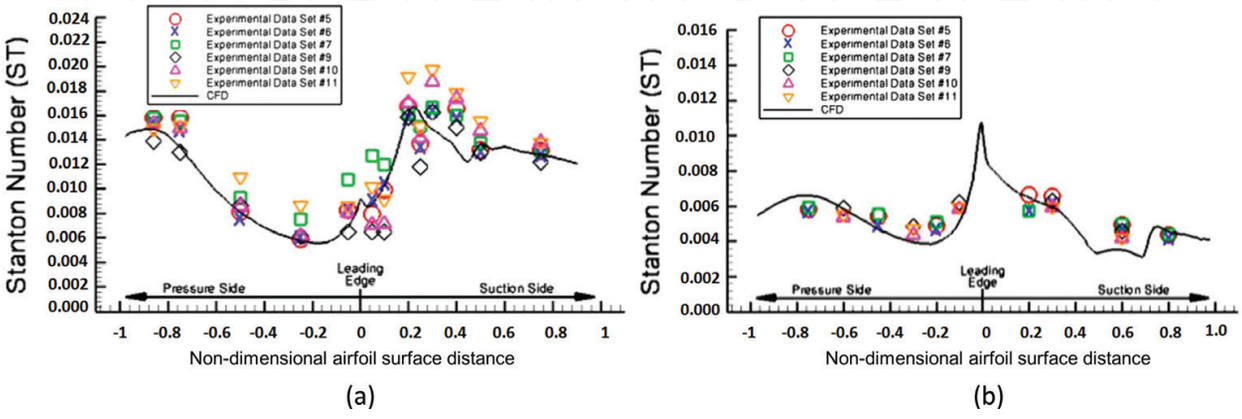

Figure 11. External heat transfer measurements at 50% span, (a) 1st stage vane, and (b) 1st stage blade. [12].

suction side until the trailing edge. However, on the pressure side, the heat transfer coefficient reduces rapidly from the leading edge, and then there is a transition to higher values until the trailing edge. These typical trends in the nonuniformity of the heat transfer coefficient are generally observed on most turbine vanes and blades. However, in addition to these generalized airofoil heat transfer distributions, actual industrial gas turbines blades are also affected by several other parameters, such as; inlet pressure and temperature profiles, airofoil shape and curvature, position of film cooling holes, thermal barrier coating roughness, transient wakes from upstream vanes, and blade passage turbulence intensity levels.

4.2. Endwall external heat loads

At the vane and blade endwall or platform, the aerodynamic flows are highly three-dimensional, transonic, and consist of areas where the hot gas flow strongly interacts with cooler rim purge and leakage flows. **Figure 12(a)** highlights the salient features of the hot gas path flow interactions on the platforms, which are largely pressure driven flows generated by the crosspassage pressure differences on the pressure and suction side of neighbouring airofoils. Over the last decade, there has been a significant experimental and numerical research effort to understand the behavior and impact of these high speed endwall flows on the platform heat transfer [4–6, 11, 16, 17]. Some of the key factors which define the platform heat transfer include the inlet profile of hot gas temperature, pressure and turbulence intensities, film cooling, platform contouring, and impact of leakage and rim purge flows.

Figure 12(b) shows the heat transfer and film cooling distributions on a first stage vane [15]. The heat transfer coefficient distribution shows that the suction side shoulder and the pressure side trailing edge regions experience the highest heat transfer coefficients, which also correspond to the areas with the highest Mach numbers. For the vane platform film cooling effectiveness without the upstream purge flows, **Figure 12(c)** shows that the measured and predicted film cooling effectiveness compares quite well, and the films remain attached to the passage wall and are very effective in cooling the platform. Due to the three-dimensional nature of the endwall flows, **Figure 12** highlights that the magnitude and directions of the local velocity, temperature, and pressure distributions play a dominant role in the heat transfer distributions on airofoil platforms.

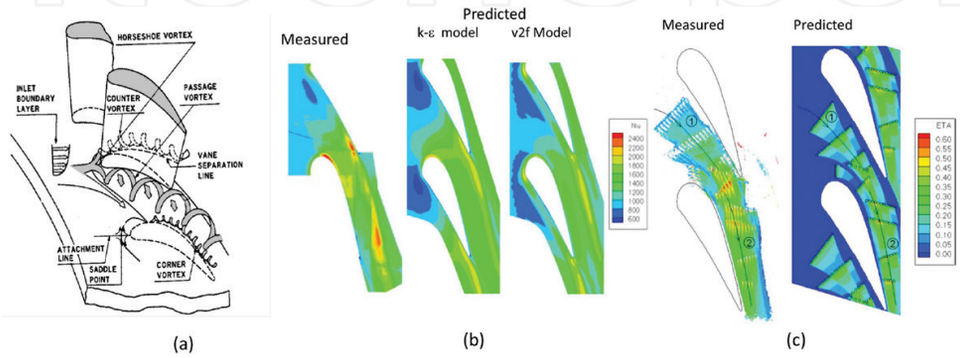

Figure 12. Endwall flow and heat transfer, (a) flow structures [14], (b) heat transfer coefficients [15], and (c) film cooling effectiveness [15].

4.3. Blade tip and endwall external heat loads

The blade tip and its neighbouring endwall regions are one of the most complex aerodynamic and heat transfer areas of the gas turbine. **Figure 13** shows some typical blade tips designs ranging from flat tips, squealers and shrouded tips, and its impact on the turbine efficiency. For flat tip and squealer tip designs, this region is dominated by the pressure driven overtip leakage flow from the airofoil pressure side to the suction side. This flow then travels through the narrow gap between the rotating blade and the static casing endwall, and subsequently interacts with the main cross passage flows to form a high speed vortex on the tip suction side. For the shrouded blade, the gas flow is from the leading to the trailing edge. The hot gas flows then interact within the rotating shroud fins with the shroud cooling air. Due to the complex flow structure and high heat loads at the blade tips, an accurate knowledge of the local aerodynamics and heat transfer is important for ensuring that the mechanical integrity of the blade tips are ensured for long operating periods, especially at higher gas turbine operating temperatures.

Figure 14 shows the sensitivity of the key parameters which influence the metal temperature of a typical squealer blade tip design. The main parameters influencing the tip metal temperatures are the hot gas temperatures and the cavity mixed temperatures. Other parameters such as the wall thickness and the heat transfer coefficients also play a major role in determining the tip metal temperatures. The heat transfer distribution on the blade tip and the endwall is highly nonuniform and driven largely by the local Mach number distributions and the tip geometry [4–6, 11, 53].

Figure 15 shows the flow distributions for two squealer tip designs and highlights the complex flow structure within the tip crown and the flow interactions between the tip leakage, main hot gas flows, and the coolant within the blade passage [18]. For these two blade tip designs, **Figure 16** also shows the measured and predicted heat transfer coefficients on the

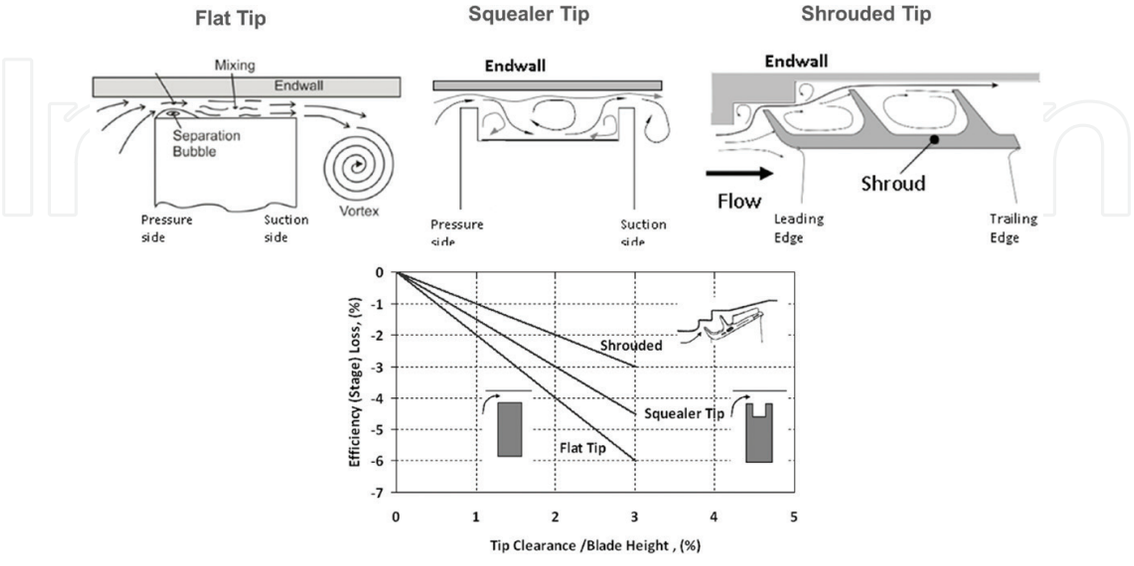

Figure 13. Typical blade tip designs and performance characteristics.

http://dx.doi.org/10.5772/67323

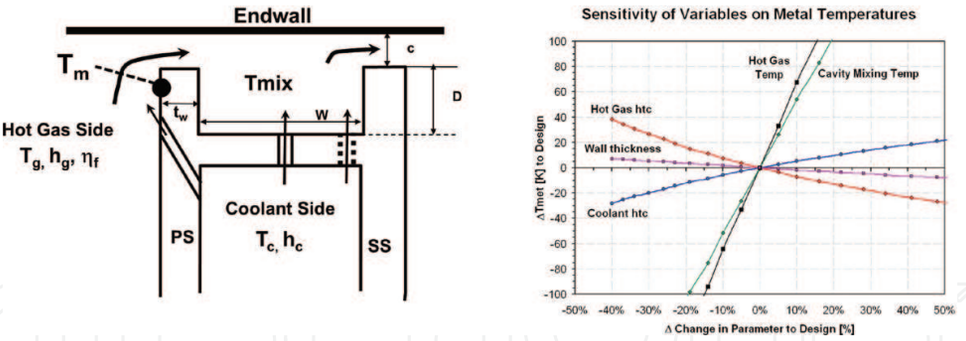

Figure 14. Sensitivity of operating conditions on blade tip heat transfer.

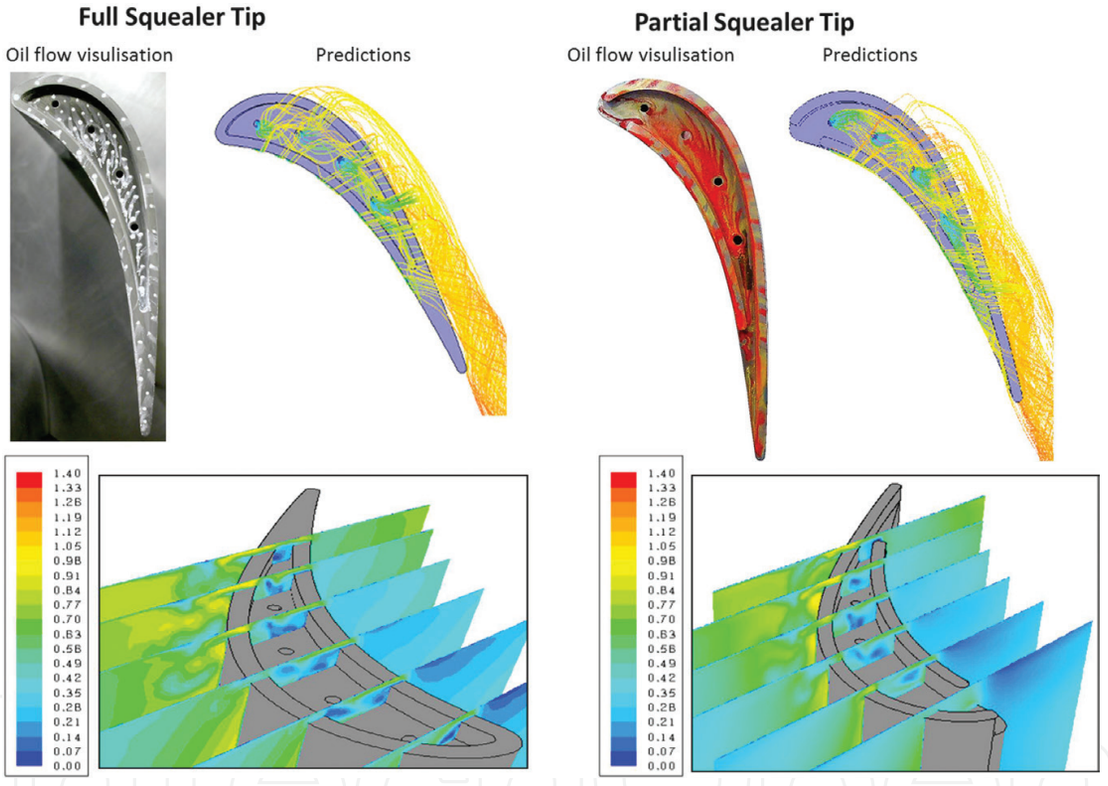

Figure 15. Flow structure and Mach number distributions for full and partial squealer blade tips [18].

blade with film cooling [18]. Both measurements and predictions show that on the blade tip, very high values exist in the leading edge regions and on the suction side rims. However, on the neighbouring endwall, the high heat transfer regions are largely location on the blade pressure side and towards the trailing edge.

4.4. Thermal barrier coatings

The use of high temperature thermal barrier coatings (TBC) for reducing the incident heat flux on both static and rotating gas turbines blades is extensive in gas turbines, particularly

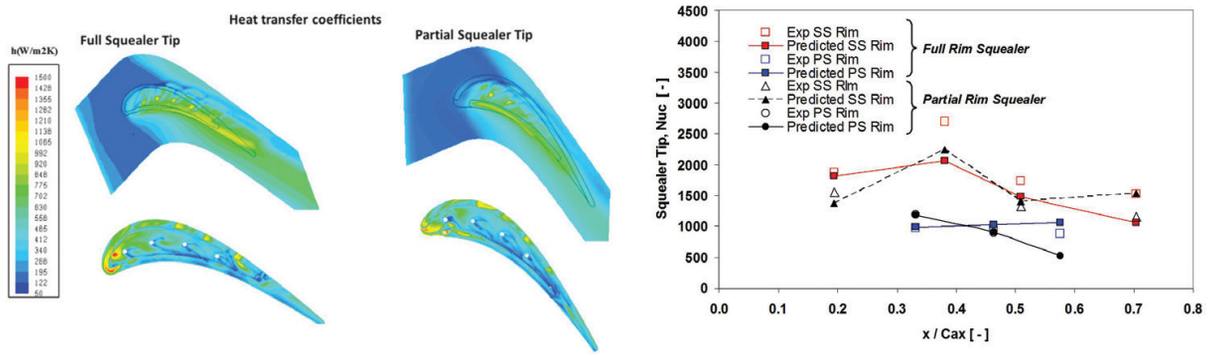

Figure 16. Heat transfer coefficient distributions on blade tip and endwall for full and partial squealer blade tips [18].

in the first and second turbine stages. There are essentially two main types of TBC, which are in widespread use in the gas turbine industry, namely air plasma sprayed (APS) and electron beam physical vapour deposition (EBPVD) [7]. For heavy duty gas turbines, the APS TBC is widely used with thickness which can range from 100 to up to 600 μm. The thermal impact of thermal barrier coatings on the turbine blade thermomechanical integrity is significant, and they therefore play an important role as a thermal protection system for gas turbine components. As highlighted previously, in the thermal analysis of turbine blades, the thermal barrier coating is generally represented as a thermal resistance to the incident heat flux, by modifying the hot gas transfer coefficient via the thermal barrier coating Biot number. **Figure 17** shows that by increasing the thickness of the thermal barrier coating and reducing its thermal conductivity, the effective hot gas heat transfer coefficient can be significantly reduced. This results in a direct reduction of the incident heat flux on the turbine blade.

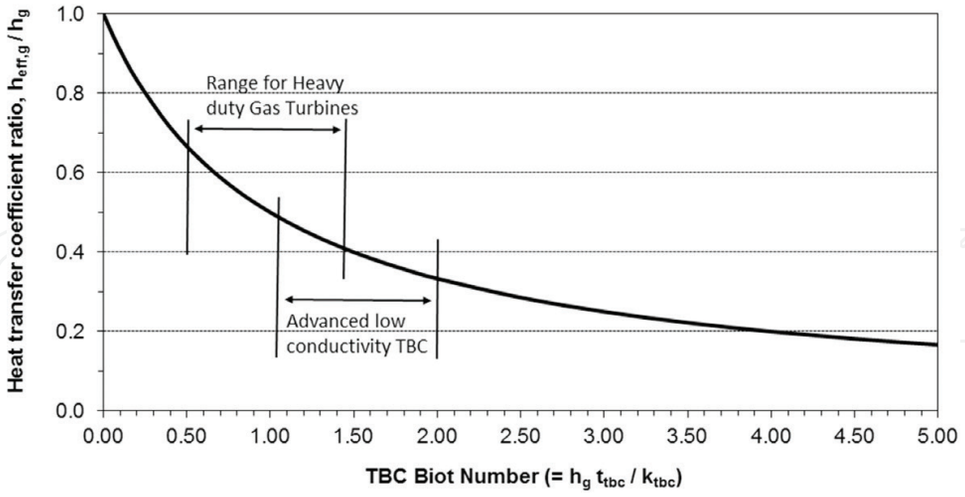

Figure 17. Effect of thermal barrier coatings (TBC) on heat transfer.

For typical heavy duty gas turbines, **Figure 17** shows that the thermal barrier coating reduces the effective heat transfer coefficient by almost 50% compared to no application of the TBC. Additionally, **Figure 17** shows that, for the new generation of advanced TBC's [6, 7], with

http://dx.doi.org/10.5772/67323

lower thermal conductivity, the effective heat transfer coefficient can be further reduced. It is clear from **Figure 17**, that thermal barrier coatings are an integral and significant part of the overall blade thermal design system.

4.5. Film Cooling

Film cooling is generally applied at different locations along the perimeter of an airofoil by rows of discrete holes, through which coolant air is discharged into the airofoil external boundary layer. The coolant, which is several hundred degrees colder than the hot gas, then creates a film of air on the airofoil surface, whose temperature is significantly lower than the surrounding hot gas. Consequently, the incident hot gas temperature for heat transfer is reduced. **Figure 18** shows an example of the application of a film row at the blade trailing edge and the key parameters which define the performances of film cooling. **Figure 19** shows that as the average film cooling effectiveness on a turbine blade is increased, the film to hot gas temperature ratio reduces and the film temperature close to the wall can be reduced by several hundred degrees relative to the surrounding hot gas temperature.

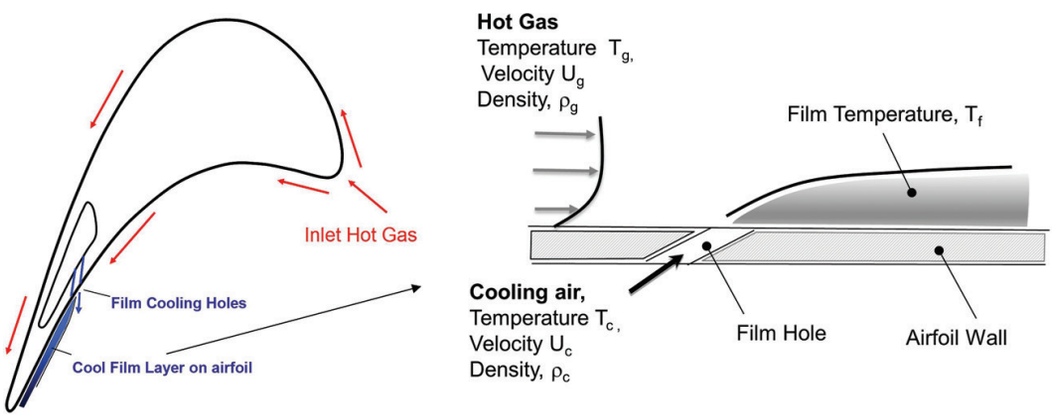

Figure 18. Film cooling of gas turbine blades.

Increasing the average film cooling effectiveness can be achieved by using many film rows, but this would be at the expense of high coolant consumption and reduced turbine efficiencies. Alternatively, increased film cooling effectiveness can also be achieved by using advanced film cooling hole designs without increasing the coolant consumption [4, 6, 11, 13, 20, 21].

The film cooling effectiveness depends on the complex aerothermal interaction between the high speed hot gas flow and the ejected film cooling jets in the external gas boundary layer. It is also dependent on several geometrical and operational parameters such as film cooling hole shape, hole angle, velocity and temperature of the ejected coolant, temperature and velocity of the surrounding hot gas, blade curvature, and local turbulence levels. As highlighted in **Figure 19**, increasing the film cooling effectiveness results in significant reduction in the film to hot gas temperature ratio, and hence there continues to be a significant research effort on developing film cooling technology due to its significant benefits in reducing local near wall

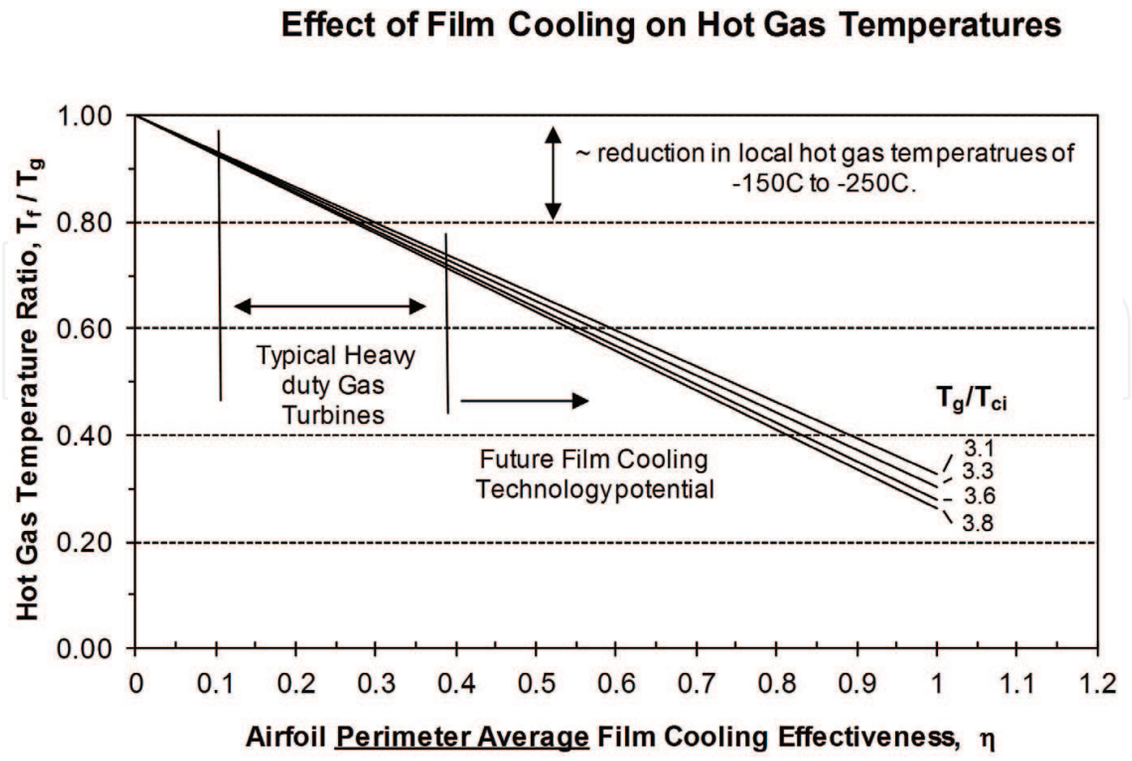

Figure 19. Effect of film cooling effectiveness on hot gas temperatures.

hot gas temperatures [4–6, 11, 16, 17, 20, 21]. Over the last decade, there has been a significant focus on airofoil, platform, and blade tip film cooling with more recent focus on advanced shapes of film cooling holes, such as three-dimensional shaped holes and trench holes. In a recent study [13], the multirow film cooling characteristic on a high lift vane and blade were demonstrated. **Figure 20** shows that the use of three-dimensional advanced fan shaped holes can provide high airofoil average film cooling effectiveness and the use of only one or two row of shaped holes located upstream of the suction side shoulder can provide high film cooling effectiveness until the trailing edge.

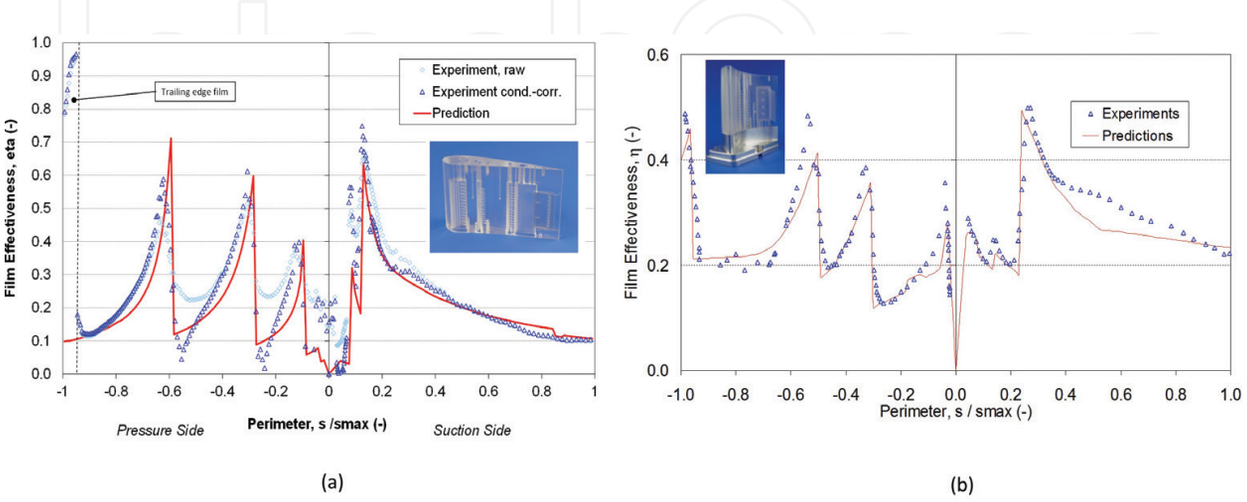

Figure 20. Multi row film cooling characteristics on a gas turbine (a) vane and (b) blade [13].

http://dx.doi.org/10.5772/67323

5. Internal heat transfer of cooled turbine airofoils

The need for the internal cooling of gas turbine blades is primarily defined by the magnitude of the incident heat load on the airofoils, which range from 0.5 to 5 MW/m^2, and the requirements of the component durability for long operating hours against thermomechanical fatigue (TMF), low cyclic fatigue (LCF), creep, oxidation, and high cyclic fatigue (HCF). While the external airofoil profile defines the airofoil aerodynamic performance, the internal cooling geometry is defined by the amount of coolant required to maintain the airofoil at a certain material temperature and the temperature gradients across critical wall sections of the airofoil. **Figure 21** shows some typical examples of turbine vane and blade cooling designs. The internal heat transfer technologies used in these vanes and blades include impingement cooling, turbulators or ribs, pin or pedestal banks, dimples, shaped internal passages, and combinations of the above cooling features.

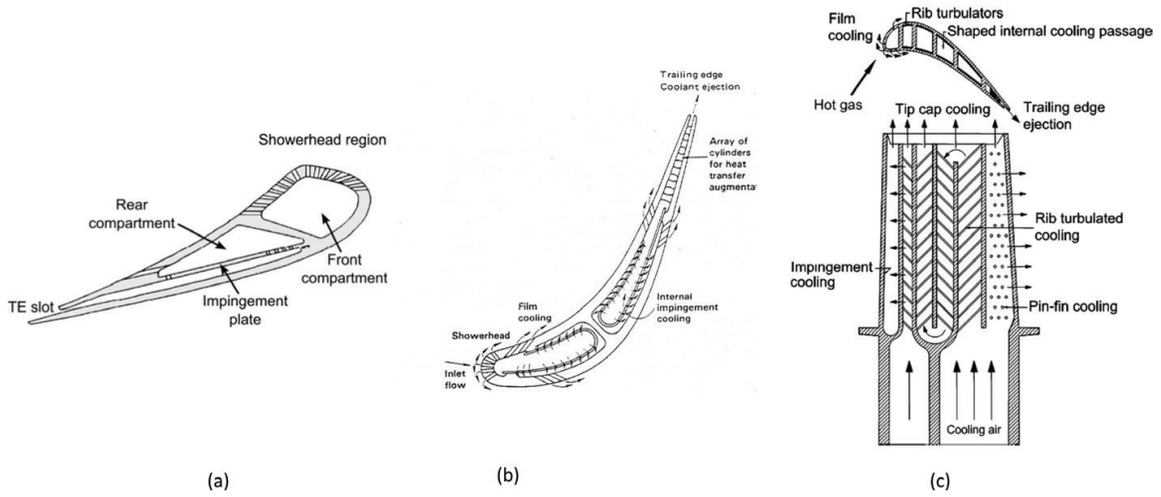

Figure 21. Typical blade cooling designs, (a) nozzle guide vane [22], (b) turbine vane [23], and (c) turbine blade [19].

5.1. Convective cooling with jet impingement

Impingement cooling is widely used for the internal cooling of gas turbine components, particularly static airofoils (vanes), heatshields (casing segments), combustor liners, and fuel nozzles. The impinging jets are generally formed through cylindrical holes in a thin wall insert, which is positioned adjacent to the airofoil inner wall that is required to be cooled. They are normally directed as a single row of jets or as multiple rows of jets, and are generally injected normal to the target surface.

For the midchord areas of airofoils, impingement cooling is designed with multiple rows of jets and is directed on the pressure and suction sides of the airofoil. The efficiency of the impingement cooling is defined by several parameters such as the standoff distance of the impingement jet relative to the target surface, the axial and radial pitch of the neighbouring impingement hole, the arrangement pattern (e.g., in-line, staggered, or other combinations), and the amount of cross-flow from the upstream impingement jets. An

overview of recent research into impingement cooling is given in Ref. [24] with impingement cooling applications detailed in Refs. [4–6, 27]. For relatively flat surfaces, **Figure 22** shows the impingement hat transfer for a flat surface with multiple impingement holes, which is based on the correlations in Ref. [25]. This figure highlights, that although jet impingement cooling is highly effective, the design of the impingement system requires careful consideration of several influencing parameters, such as the standoff distance from the target surface, the axial and lateral pitch of the impingement holes and the amount of crossflow from upstream jets.

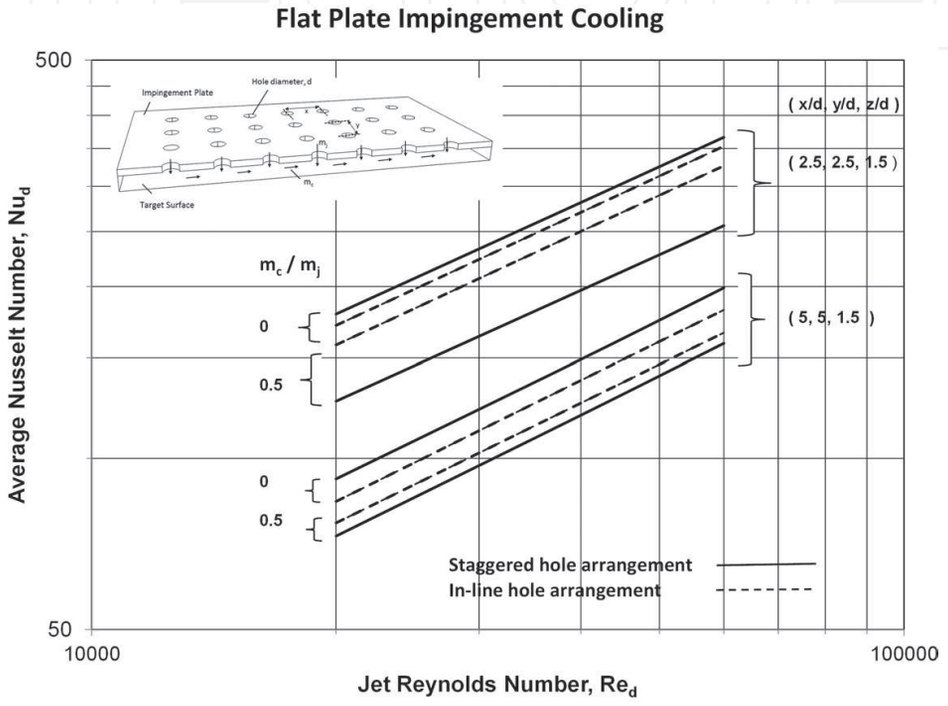

Figure 22. Impingement heat transfer with multiple rows on flat target surfaces.

Airofoil curved leading edges are normally subjected to very high heat loads, and at these locations, internal impingement cooling in combination with turbulators and film cooling is quite common. **Figure 23** shows the dependency of the standoff distance and the leading edge curvature on the coolant Nusselt numbers at varying Reynolds numbers, based on the correlation in Ref. [26]. Highest stagnation heat transfer can be achieved if the jets are arranged very close to the target surface and the highest average heat transfer are achieved for airofoils with small internal leading edge diameters. At the internal leading edges, there are also several other additional factors that influence the airofoil heat transfer, such as showerhead film cooling, turbulators, surface roughness, and the amount of impingement crossflows [4–6].

More recently, there have been several studies on the use of narrow channel impingement passages and inclined impingement jets in variable shaped passages. Such design configurations can provide higher internal heat transfers and have been mainly driven by the introduction of near wall cooling features in gas turbine blades. Such configurations can be manufactured with 3D printing technologies such as selective laser melting (SLM) and direct laser melting (DLM), which allows greater manufacturing flexibility with geometrically complex cooling passages.

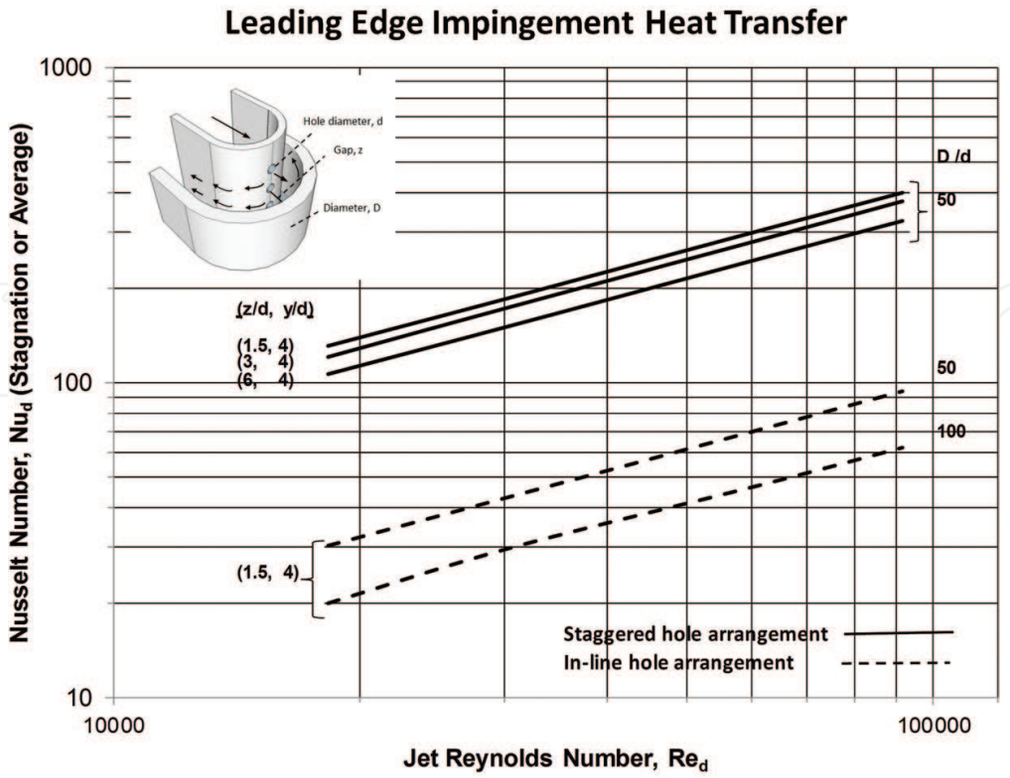

Figure 23. Impingement heat transfer on curved leading edge surface.

For narrow channel impingement, it was recently highlighted in Ref. [28] that in addition to the high heat transfer from the target surface, the heat transfer from the impingement cavity side walls can also be significant. **Figure 24** shows that for a narrow channel with in-line impingement holes, the heat transfer from the side walls can be up to 50% of that from the target plate.

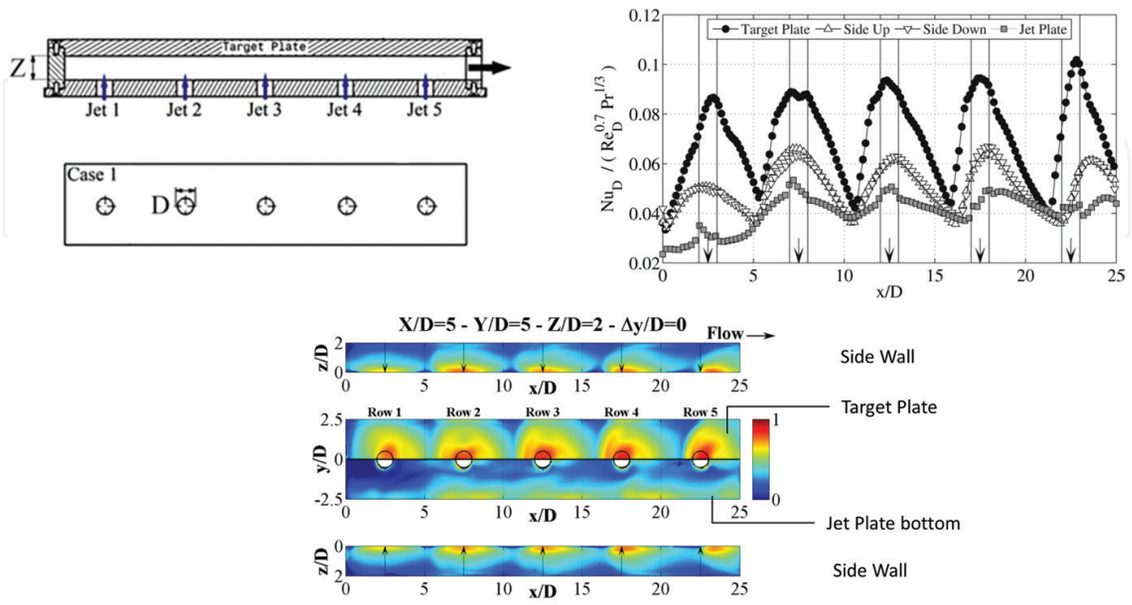

Figure 24. Impingement heat transfer in narrow channel passages [28].

The use of inclined impingement jets on shaped turbulators in irregular shaped passages can also result in very high heat transfer. In a recent study [29, 30], and as shown in **Figure 25**, it was highlighted that directed inclined impingement can result in relatively high heat transfers from the target walls and additionally produces intense convective fluid mixing within the passage. In a turbine blade, such a combination can result in greater total heat removal by the coolant from the hot airofoil walls. The use of directed impinging cooling jets in the leading edge passages was demonstrated in Ref. [31]. **Figure 26** shows that directing a double impingement jets on a curve leading edge with showerhead cooling results in high heat transfer coefficients at the pressure and suction surfaces, and additionally generates significant turbulent mixing within the leading edge passage.

Based on the many different design variations of impingement cooling, it is expected that impingement cooling systems will continue to play a significant role in gas turbine heat transfer technology.

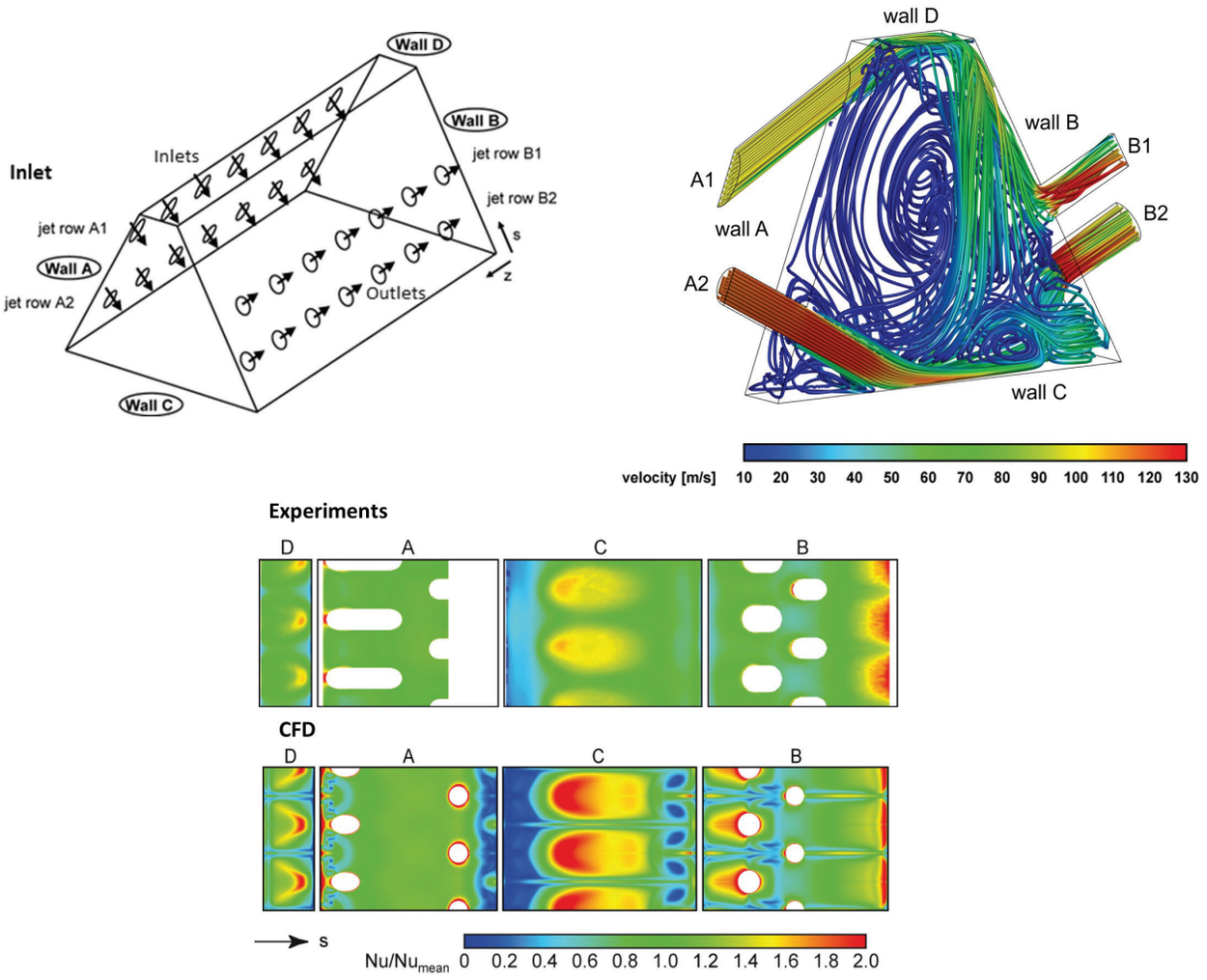

Figure 25. Impingement heat transfer in irregular passages [29, 30].

http://dx.doi.org/10.5772/67323

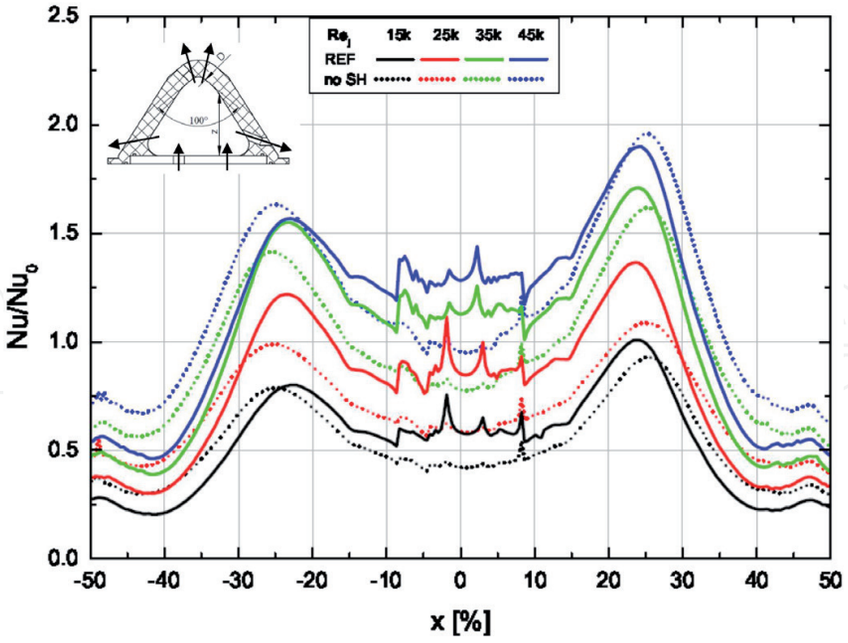

Figure 26. Impingement heat transfer in leading edge channels [31].

5.2. Convective cooling with turbulators

The use of ribs or turbulators for cooling gas turbine blades is a major heat transfer technology and has been employed largely in rotating blades with radial passages as shown in **Figure 27**. The passages are typically arranged as multiple radial passages and commonly referred to as serpentine passages or multipass systems, and the turbulators are generally designed on the pressure and suction surfaces of the passages. The key function of the turbulators is to create regions of flow separation downstream of the turbulators, which promotes intense regions of turbulence, secondary flows, and rapid mixing between the air warmed by the heated walls and the core coolant flow. The nature of the flow structure and the amount of heat transferred in the passages with turbulators is dependent significantly on the turbulator shape, configuration pitch, height, angle of orientation, flow Reynolds number, rotation, passage shape, and its aspect ratio. There has been a significant amount of research conducted on the application of turbulators in gas turbine blades, including the effects of rotation, shapes, sizes, orientation, entrance length effects, position of film cooling holes, presence of bends and other enhancement devices, and operating parameters [4–6, 19, 33, 52].

To assess the relative impact of different turbulators on the heat transfer and frictional characteristics, **Figure 27** shows the ribbed wall heat transfer and passage frictional enhancement of turbulators in various aspect ratio passages, based on the correlation in Ref. [32]. **Figure 27** highlights that the turbulator angle and the shape of the passage have a major effect on both the passage heat transfer and pressure loss. Although smaller aspect ratio ducts (W/H = 0.25) generally give higher heat transfer enhancement on the ribbed walls and lower pressure losses, the passage average heat transfer values can be lower due to the larger perimeter of the nonribbed walls, which have much lower heat transfer enhancement. Although the results shown in **Figure 27**

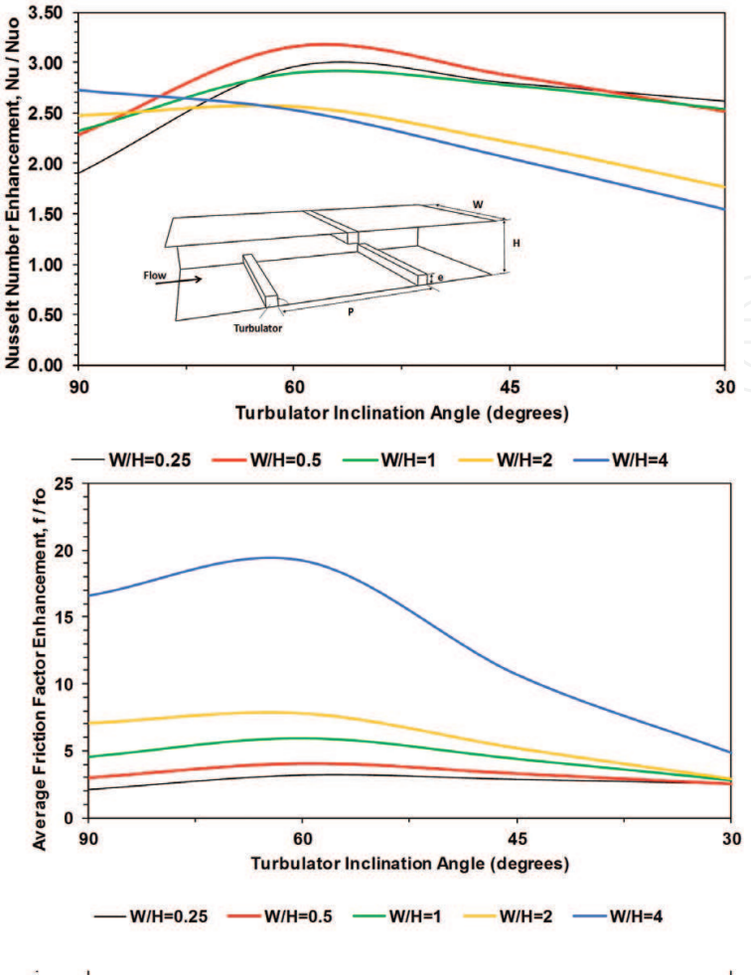

Figure 27. Passage heat transfer and frictional losses due to turbulator design and passage shape.

are for low Reynolds number, and with idealized geometry, care needs to be taken when implementing such results in real turbine blades with cast geometries, where the dimensions, shape, and position of the turbulators can be different from the predicted idealized geometries.

The impact of rotation on the heat transfer from gas turbine blades can be significant and is dependent on several additional parameters such as the rotational and buoyancy numbers [34, 35]. **Figure 28** shows a schematic overview of the impact of rotation on the flow field in a two-pass rotating passage of a gas turbine blade. Under rotating conditions, Coriolis and buoyancy effects can significantly alter the temperature and velocity profiles within the passages.

In a study from Ref. [35], **Figure 28** shows that with the coolant flowing radially upwards, the heat transfer with increasing rotation numbers, increases on the pressure side and reduces on the suction surfaces. Similarly, when the coolant flows radially inwards, the heat transfer increases on the suction side and reduces on the pressure side, especially for smooth passages. However, for passages with turbulators, the turbulators tend to dampen the effect of rotation and the heat transfer enhancement on the pressure and suction sides. This overall trend of rotation with different type of passages and turbulators has been observed by several studies [33–35], and these effects play an important role in the design of gas turbine blades.

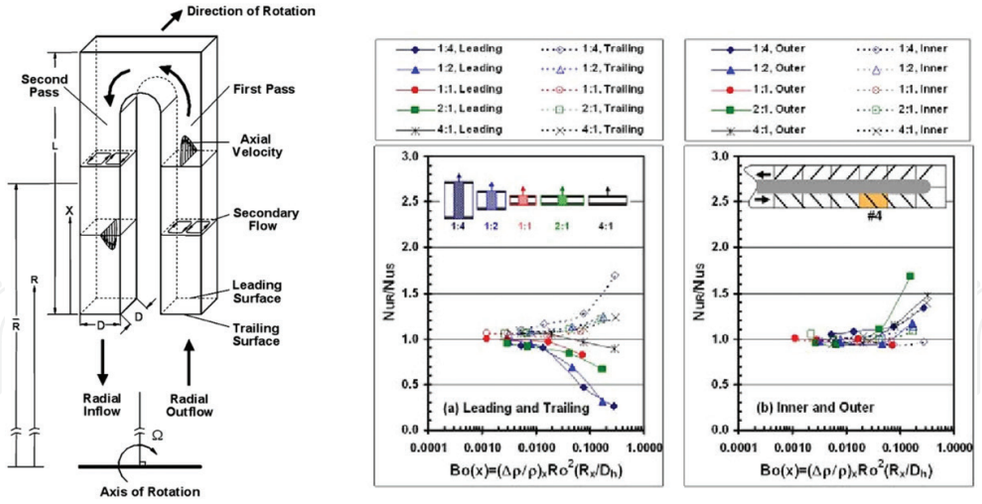

Figure 28. Impact of blade rotation on passage heat transfer [6, 19, 35].

The trailing edge regions of rotating blades are in general the most difficult to thermally design, largely due to the thin airofoil geometry, complex internal flow geometry, and the coolant flow conditions. The trailing edge region generally consists of coolant passages with very high aspect ratios, typically between 4 and 7, and which have cooling features such as turbulator and pedestals. Previous studies in such triangular and wedge-shaped passages with various turbulator shapes have been investigated by Refs. [36, 37, 38, 39]. They reported significant variation in the heat transfer distribution in both stationary and rotating cases. In a recent study [40], it has been shown that the impact of high Reynolds number typically found in heavy duty gas turbines can have a significant effect on the overall thermal performances of angled, broken, and chevron turbulators in a very large aspect ratio passage. **Figure 29**

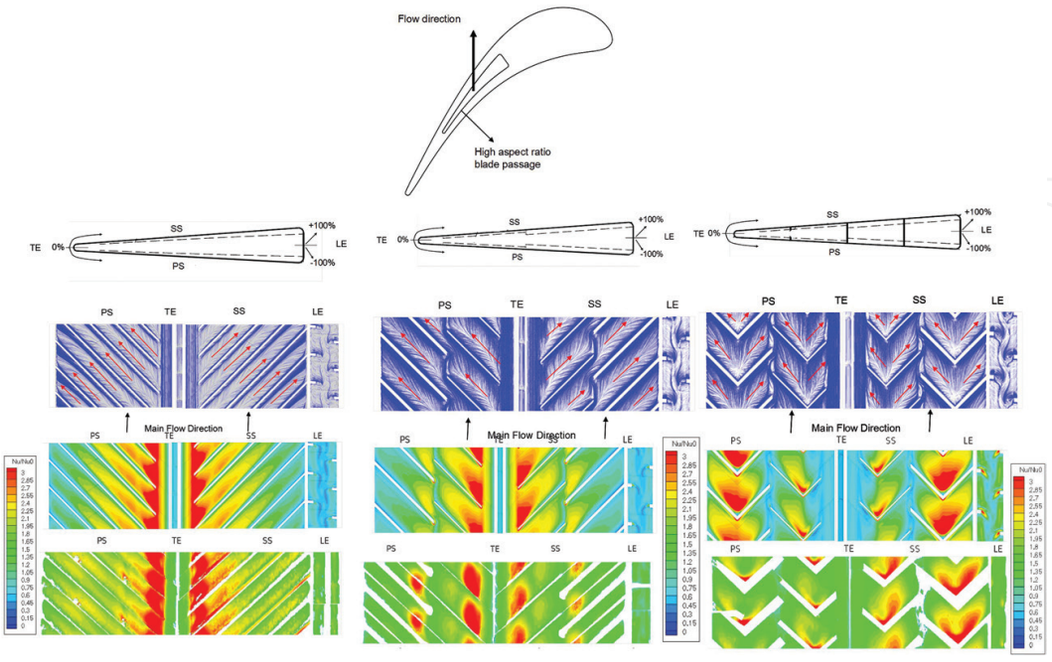

Figure 29. Impact of turbulator design in trailing edge passage [40].

shows the complex flow structures and the high three-dimensional heat transfer distribution which exist within the high aspect ratio triangular passages with different turbulator shapes. **Figure 30** shows the comparison of the average thermal performances and shows that at high Reynolds numbers, the differences between the various designs are very similar. When considering the investigated turbulator design for gas turbine cooling applications, all three configurations show comparable levels of heat transfer performances.

For leading edge passages of gas turbine blades, the application of turbulators is also widespread. However, due to the leading edge geometry, the heat transfer is significantly different to that in midchord or trailing edge passages. Several studies show the impact of the turbulator geometry on the overall heat transfer in gas turbine blade leading edges [33, 41–43]. In a recent study by Saxer-Felici et al. [44], several turbulator geometries were tested at engine representative Reynolds numbers. **Figure 31** shows that the flow structure is significantly modified due to the presence of the turbulators, and this dominates the strength and distribution of the local and average heat transfer coefficients.

The final selection and implementation of turbulator designs in a turbine blade are dependent on several additional complex requirements. These include blade metal temperature, metal temperature gradients, cooling flow pressure margins, and the amount of required cooling flow. A further key criterion is for the fulfilment of the blade mechanical integrity, which is determined by the blade low cycle fatigue and creep behaviour, both of which are driven by the local metal temperature gradients and the absolute metal temperatures. An optimal balance of these factors is therefore needed to select the best turbulator concept for a blade design system.

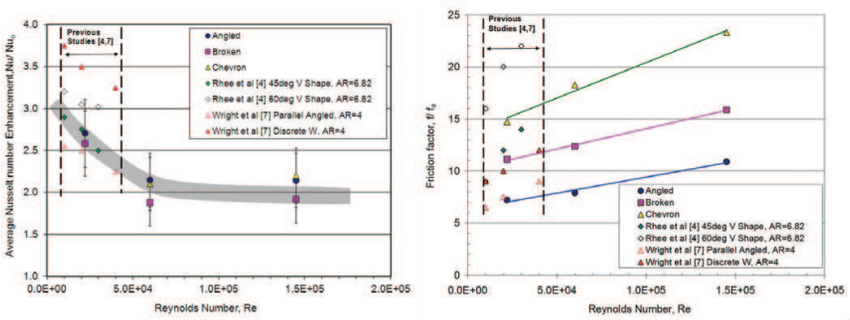

Figure 30. Average heat transfer and frictional loss in trailing edge passages [40].

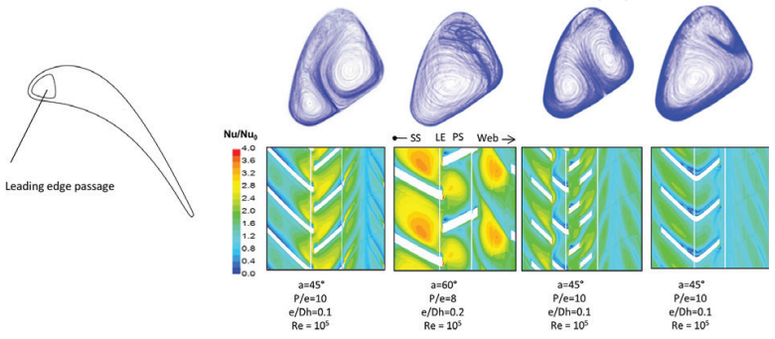

Figure 31. Heat transfer in leading edge passages [44].

http://dx.doi.org/10.5772/67323

5.3. Convective cooling with pins and pedestals

The use of pins and pedestals for enhancing the internal heat transfer in gas turbine blades and vanes is quite common particularly at the airofoil trailing edges, which generally demands aerodynamically small wedge angles and thin trailing edge diameters. Pin banks and pedestals are sometimes the only method of cooling in the space constrained narrow, converging trailing edges. They are also preferred from a manufacturing point as they tend to offer structural stability for casting. An additional advantage is that the pin banks also provide good mechanical integrity of the blades due to the robust structural support between the pressure and suction surfaces of the airofoil. In general, the pins are cylindrical in shape, tend to be thick relative to their height, has fillets imposed at the interface with blade walls, and are typically arranged in a staggered pattern. Although they provide high heat transfer due to a combination of high heat transfer coefficients from the base wall and the pins, they also entail high pressure losses. The latter disadvantage is generally not a major issue for convectively cooled blades, where there is availability of higher coolant pressure ratios relative to the surrounding hot gas pressure at the blade trailing edge.

There have been a large number of heat transfer studies on pin banks which have addressed the influences of pin geometry, channel shape, arrangements, pin shapes and combination of pins with dimples and turbulators [45–49]. For straight passages with pin banks, the local heat transfer generally increases from the first row of pins until the second to third row and then starts to decrease. For converging ducts, **Figure 32** shows that with a converging duct, the heat transfer increases in the downstream section. Additionally, by using a thicker pin in the rear portion of the passage, further increase in heat transfer can be achieved, which is driven by the increased Reynolds number.

In a recent study [50], several pin fin configurations were investigated in a trailing edge converging channel which consisted of cylindrical pins, conical pins, and a hybrid cyl-

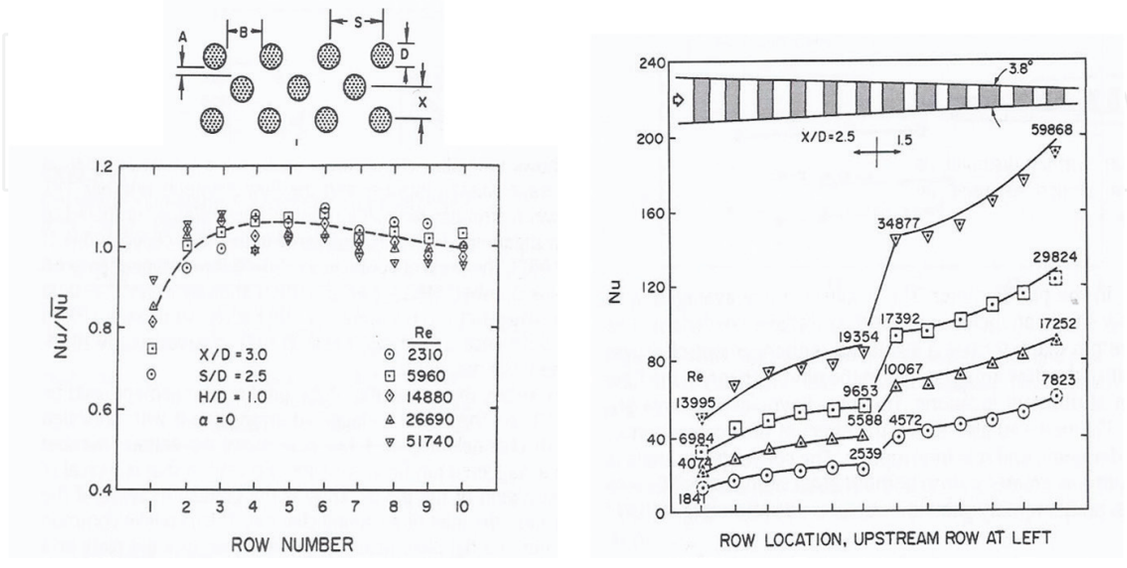

Figure 32. Heat transfer in pin banks and pedestals [45, 46].

inder pin/turbulator configuration. **Figure 33** highlights the investigated geometries. **Figure 34** shows from both predictions and measurements that the flow is highly turbulent downstream of the pins and that the complex heat transfer distribution exists on both the endwall and the pins. High levels of local heat transfer occur at the leading edge stagnation point of the pins and at the leading edge endwall. Lower heat transfer coefficients were predicted and measured in the wake region of the pin trailing edge. Laterally, averaged local distributions of the heat transfer enhancement are shown in **Figure 34** for the tested geometries, and the nonuniform nature of the heat transfer in the pin banks are further highlighted.

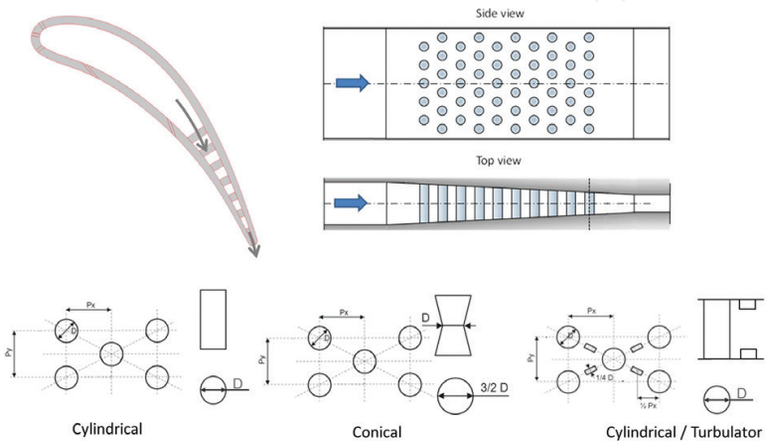

Figure 33. Trailing edge passages with different pin bank configurations [45, 46].

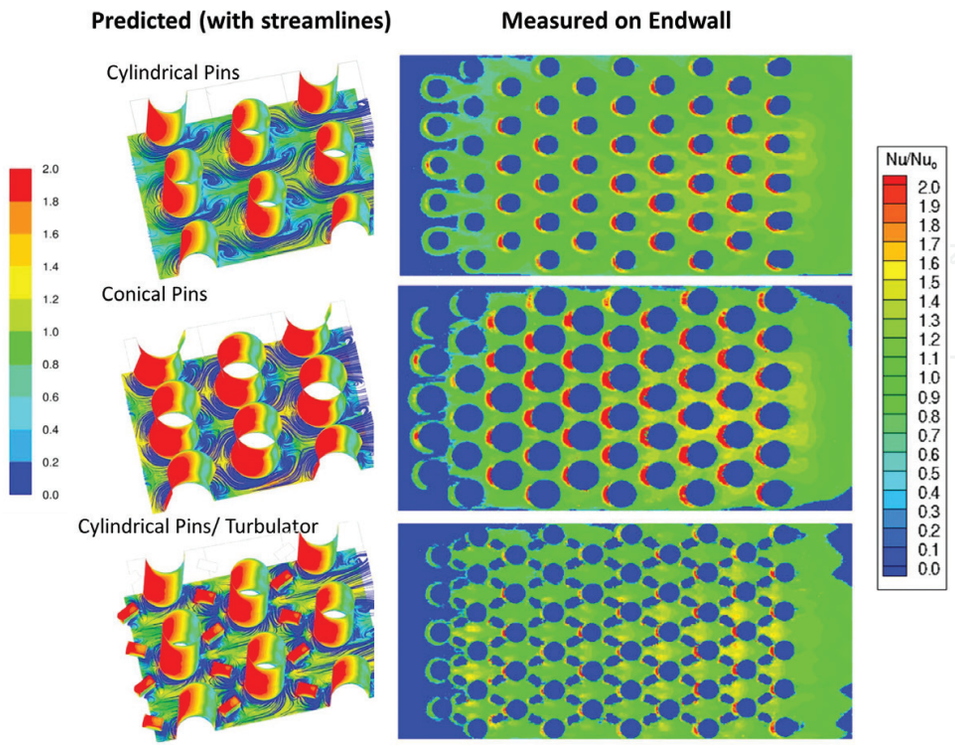

Figure 34. Heat transfer in trailing edge passages with different pin bank configurations [50].

http://dx.doi.org/10.5772/67323

6. Gas turbine heat transfer validation

One key aspect in the aerothermal design of gas turbine airofoils is the validation of the airofoil thermal performances under engine operating conditions. The design aspect outlined in the previous sections focused on individual design features such as film cooling, turbulators, pins, and impingement. For the overall validation of the cooling system of turbine blades and vanes, static perspex model testing is very common and is generally scaled to match engine operating Reynolds and Mach numbers. Typically, methods for the heat transfer testing include thermochromic liquid crystals (TLC) with embedded pressure and temperature sensors, which together provide a full map of the internal heat transfer and pressure drop characteristic of the blade cooling system for a range of flow conditions. **Figure 35** shows some examples of perspex models used for heat transfer testing.

For the testing and validation of the external film cooling, cascade test rigs are generally employed to validate the external aerodynamics and the film cooling performances. The blade or vane models are generally scaled to engine geometry and the cascade is operated at engine Mach and Reynolds number conditions. **Figure 36** shows an example of a first stage vane and

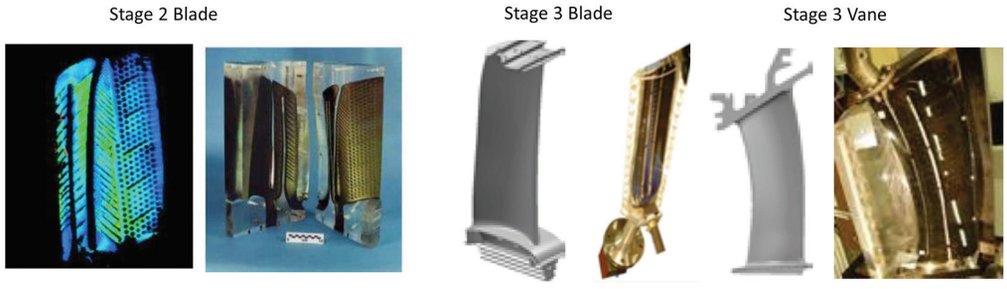

Figure 35. Perspex model testing of gas turbine blades and vanes [2].

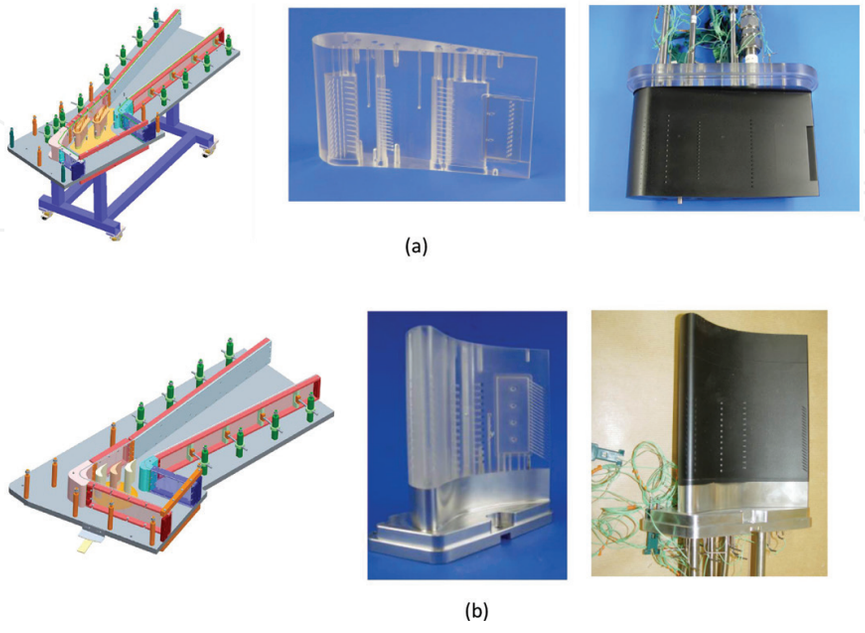

Figure 36. High speed cascade model testing of gas turbine components, (a) Turbine Vanes, (b) Turbine Blades, [13].

blade cascade with test models. These rigs enable measurements of heat transfer coefficients, film cooling effectiveness, airofoil pressure distributions, and oil flow visualization at engine representative operating conditions.

In addition to the above tests, the final validation test is conducted in a test gas turbine, which effectively represents the full operating boundary conditions that are prevalent for the entire operating range. For full engine testing, the measurement techniques employed include thermal paint, thermocouples, thermos-crystals, pyrometers, pressure taps, Kiel-Temperature and pressure probes and several other operating instrumentations. **Figure 37** shows a gas turbine with the airofoils painted with thermal paint and the additional instrumentation required to validate and monitor the airofoil and engine performances.

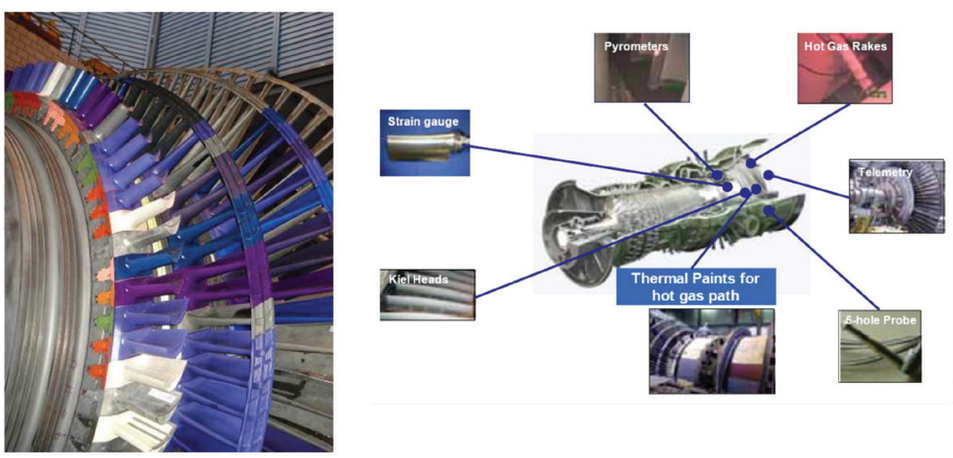

Figure 37. Gas turbine test engine and instrumentation [2].

7. Conclusion

The aerothermal design of gas turbine components has progressed at a rapid pace in the last decade with all gas turbine manufacturers, in order to obtain higher thermodynamic efficiencies. This has been achieved by using higher turbine inlet temperatures and pressures, advanced turbine aerodynamics, efficient cooling systems for turbine airofoils and advanced high temperature alloys, metallic coatings, and ceramic thermal barrier coatings.

In this chapter, some of the basic heat transfer phenomenon associated with both the external hot gas side and the coolant internal flows in turbine airofoils has been outlined. The external hot gas side heat transfer is largely driven by the unsteady and transonic high pressure and high temperature aerodynamic flows. By establishing the hot gas side external heat loads, which generally varies with different turbine design, it is possible to design for efficient airofoil internal cooling systems. The gas turbine airofoil internal cooling systems are however complex and varied in design, particularly with static and rotating airofoils. The internal cooling design of airofoils generally involves integration of several technology features such

as film cooling, three-dimensional turbulators, pedestals, impingement cooling, and thermal barrier coatings.

Due to the complexity of the heat transfer phenomenon associated with gas turbine airofoils, it is also relatively common that final airofoil designs are thermally validated in several validation carriers which are representative of engine conditions. These validation carriers include high speed cascade rigs, scaled perspex models, airflow and qualitative heat transfer flow benches, and gas turbine test engines.

Author details

Shailendra Naik

Address all correspondence to: shailendra.naik@ansaldoenergia.com

Ansaldo Energia, Baden, Switzerland

References

[1] R.H. Kehlhofer, J. Warner, H. Nielsen, R. Bachmann, Combined Cycle Gas - Steam Turbine Power Plant, 2nd Edition, Pen Well Publishing Company, Oklahoma, ISBN 0.87814-736-5, 1998.

[2] S. Naik, T. Sommer, M. Schnieder, Aero-thermal design and validation of an advanced turbine, Proceedings of ASME Turbo-Expo Power for Land, Sea and Air, Paper GT2012-69761, June 5-7, Copenhagen, Denmark, 2012.

[3] S. Can Gülen. Étude on gas turbine combined cycle power plant—next 20 years. Journal of Engineering for Gas Turbines and Power, **138**(5) 051701, pp 1-10, 2015.

[4] J.C. Han, S. Dutta, S. Ekkad, Editors, Gas turbine heat transfer and cooling technology, Taylor and Francis, ISBN 1-565032-841-X, 2000.

[5] C. Lechner, J. Seume, Editors, Stationäre gasturbinen, Springer-Verlag, Heidelberg, ISBN 3 540-42831-3, 2003.

[6] The Gas Turbine Handbook, Ed. R. Dennis, published by National Energy Technology Laboratory, Department Of Energy, Morgantown, WV, USA, 2006.

[7] D.R. Clarke, M. Oechsner, N.P. Padture, Thermal-barrier coatings for more efficient gas-turbine engines, MRS Bulletin. 2012;**37**(10).

[8] W. Krebs, J. Hellat, A. Eroglu, Technische Verbrennungssystem, Ch. In C. Lechner and J. Seume, Editors, Stationäre Gasturbinen, Springer-Verlag, Heidelberg, ISBN 3-540-42831-3, 2003.

[9] T. R. Kingston, Rapid design, analysis and optimisation of cooled turbine blades, Paper ISABE 2015-20275, 22nd International Symposium on Air Breathing Engines, October 23–25 2015, Phoenix, Arizon, USA.

[10] J. Krueckels, T. Arzel, T.R. Kingston, M. Schnieder, Turbine blade thermal design process enhancements for Increased firing temperatures and reduced coolant flow, Proceedings of ASME Turbo-Expo Power for Land, Sea and Air, Paper GT2007-27457, May 14–17, Montreal, Canada, 2007.

[11] M.G. Dunn, Convective heat transfer and aerodynamics in axial flow turbines, ASME Journal of Turbomachinery. 2001;**123**:637.

[12] J.A. Tallman, C.W. Haldeman, M.G. Dunn, A.K. Tolpadi, R.F. Bergholz, Heat transfer measurements and predictions for a modern, high pressure transonic turbine including endwalls, Transactions of the ASME, Journal of Turbomachinery. 2009;**131**.

[13] S. Naik, J. Krueckels, M.Gritsch, M. Schnieder, Multi-row film cooling perfomances of a high lift blade and vane, Transactions of ASME, Journal of Turbomachinery. 2014;**136**:051003-1.

[14] K. Takeishi, M. Matsuura, S. Aoki, T. Sato, An experimental study of heat transfer and film cooling on low aspect ratio turbine nozzles, Trans. ASME, J. Turbomach, 112(3), pp 488-496, 2008.

[15] J. Krueckels, W. Colban, M. Gritsch, M. Schnieder, Validation of a first vane platform cooling design, Proceedings of ASME Turbo Expo, GT2011-45252, June 6–10, Vancouver, Canada, 2011

[16] Barigozzi, G., Benzoni, G., Franchini, G., Perdichizzi, A., "Fan-shaped hole effects on the aero-thermal performance of a film cooled endwall," Transactions of the ASME, Journal of Turbomachinery. 2006;**128**:43–52.

[17] Colban, W., Thole, K.A., Haendler, M., A comparison of cylindrical and fan-shaped film-cooling holes on a vane endwall at low and high freestream turbulence levels, Trans. of ASME, Journal of Turbomachinery. **130**(3), 031007, pp 1–9, 2008.

[18] S. Naik, C. Georgakis, T. Hofer, D. Lengani, Heat transfer and film cooling of blade tips and endwalls, Transactions of ASME, Journal of Turbomachinery. 2012:**134**:041004-1.

[19] J.C. Han, Recent advances in turbine blade cooling, International Journal of Rotating Machinery. 2004;**10**(6):443–457.

[20] J.C. Han, A.P. Rallabandi, Turbine film cooling using PSP technique, Frontiers in Heat and Mass Transfer. 2010;**1**:013001.

[21] S. Baldauf, M. Scheurlen, A. Schulz, S. Wittig, Correlation of film-cooling effectiveness from thermographic measurements at enginelike conditions, ASME Journal of Turbomachinery. 2002;**124**:686.

[22] S. Luquel, J. Batstone, D.R.H. Gillespie,T. Povey, and E. Romer, Full thermal experimenta assessment of a dendritic turbine vane cooling scheme, Transactions of The ASME, Journal of Turbomachinery. 2014;**136**:021011.

[23] J.R. Taylor, Heat Transfer Phenomena in Gas Turbines, Proceedings of ASME International Gas Turbine Conference, Paper 80-GT-172, March 10-13, New Orleans, USA, 1980.

[24] B. Weigand and S. Spring, Multiple jet impingement—a review, Heat Transfer Research. 2011;**42**(2):101–142.

[25] L.W. Florschuetz, D.E. Metzger, C.C. Su, Heat transfer characteristics for jet array impingement with initial crossflow, ASME Jorunal of Heat Transfer. 1984;**106**:34–41.

[26] R.E. Chupp, H.E. Helms, P.W. McFadden, T.R. Brown, Evaluation of internal heat transfer coefficients for impingement cooled turbine airfoils, Proceedings of AIAA, 4th Propulsion Joint Specialist Conference, Paper AIAA 68-564, 10–14 June, Ohio, USA,1968.

[27] M.E. Taslim, L. Setayeshgar, S.D. Spring, An Experimental Evaluation of Advanced Leading Edge Impingement Cooling Concepts, Trans of ASME, Journal of Turbomachinery, 123(1), pp 147-153, 2000.

[28] A. Terzis, P. Ott, J. Wolfersdorf, B. Weigand, M. Cochet, Detailed heat transfer distributions of narrow impingement channels for cast-in turbine airfoils, Transactions of ASME, Journal of Turbomachinery. 2014;**136**:091011-1.

[29] F. Hoefler, S. Schueren, J. Wolfersdorf, and S. Naik, Heat transfer characteristics of an oblique jet impingement configuration in a passage with ribbed surfaces, Transactions of ASME, Journal of Turbomachinery. 2011;**134**.

[30] S. Schueren, F. Hoefler, J. Wolfersdorf, S. Naik, Heat transfer in an oblique jet impingement configuration with varying jet geometries, Transactions of ASME, Journal of Turbomachinery. 2012;**135**(2).

[31] B. Facchini, F. Maiuolo, L. Tarchi, N. Ohlendorf, Experimental investigation on the heat transfer of a leading edge cooling system: effects of jet-to-jet spacing and showerhead extraction, Proceedings of ASME Turbo Expo 2013, GT2013-94759, June 3–7, San Antonio, Texas, USA, 2013.

[32] J.C. Han, J.S. Park, 1988. Developing heat transfer in rectangular channels with rib turbulators. International Journal of Heat and Mass Transfer. 1988;**31**(1):183–195.

[33] P. Ligrani, Heat transfer augmentation technologies for internal cooling of turbine components of gas turbine engines, International Journal of Rotating Machinery, v2013, Article ID 275653, 32 pages, 2013.

[34] B.V. Johnson, J.H. Wagner, G.D. Steuber, F.C. Yeh, "heat transfer in rotating serpentine passages with trips skewed to the flow," ASME Paper No. 92-GT-191, ASME Journal of Turbomachinery. 1992;**116**:113–123.

[35] W.L. Fu, L.M. Wright, J.C. Han, Rotational buoyancy effects on heat transfer in five different aspect-ratio rectangular channels with smooth walls and 45 degree ribbed walls, Transaction of ASME Journal of Heat Transfer. 2006;**128**(11):1130–1141.

[36] D.H. Rhee, D.H. Lee, H.H. Cho, Effects of duct aspect ratios on heat/mass transfer with discrete V-shaped ribs, Proceedings of ASME Turbo-Expo Power for Land,Sea and Air, Paper GT2003-38622, June 16-19, Atlanta, USA, 2003.

[37] R. Kiml, S. Mochizuki, A. Murata, J. Sulitka, Rib-induced secondary flow structures inside a high aspect ratio trapezoidal channel, Proceedings of the International Gas Turbine Congress, Paper IGTC2003Tokyo-078, Nov 2-7, Tokyo, Japan, 2003.

[38] L.M. Wright, Y.-H. Liu, J.-C. Han, S. Chopra, Heat transfer in trailing edge, wedge shaped cooling channels under high rotation numbers, ASME Journal of Heat Transfer. 2008;**130**.

[39] M.E. Taslim, T. Li, and S.D. Spring, "Experimental study of the effects of bleed holes on heat transfer and pressure drop in trapezoidal passages with tapered turbulator," ASME Journal of Turbomachinery. 1995;**117**:pp. 281–289.

[40] S. Naik, S. Retzko, and M. Gritsch, Impact of turbulator design on the heat transfer in a high aspect ratio passage of a turbine blade, Proceedings of ASME Turbo-Expo for Land, Sea and Air, Paper GT2014-25841, June 16-20, Duesseldorf, Germany, 2014.

[41] M.E. Taslim, T. Li, S.D. Spring, "Measurements of heat transfer coefficients and friction factors in rib-roughened channels simulating leading-edge cavities of a modern turbine blade". Transactions of The ASME, Journal of Turbomachinery. 1997;**119**:602–609.

[42] N. Domaschke, J. von Wolfersdorf, K. Semmel, Heat transfer and pressure drop measurements in a rib leading edge channel, Trans of ASME, Journal of Turbomachinery, 134(6), 061006, pp 1-9, 2012.

[43] C. LeBlanc, S.V. Ekkad, T. Lambert, V. Rajendran, Detailed heat transfer distributions in engine similar cooling channels for a turbine rotor blade with different rib orientations, Trans of ASME, Journal of Turbomachinery, 135(1), 011034, 2012.

[44] H. Saxer-Felici, S. Naik, M. Gritsch, Heat transfer enhancement for a turbine blade leading edge passage using various turbulator geometries, Proceedings of ASME Turbo-Expo for Land, Sea and Air, Paper GT2014-26130, June 16-20, Duesseldorf, Germany, 2014.

[45] J. Armstrong D. Winstanley, "A review of staggered array pin fin heat transfer for turbine cooling applications," Transaction of the ASME, Journal of Turbomachinery. 1988;**110**:94–103.

[46] D.E. Metzger, W.B. Shepard, S.W. Haley, Row resolved heat transfer variations in pin/fin arrays including effects of non-uniform arrays and flow convergence, Proceedings of ASME Turbo-Expo for Land, Sea and Air, Paper 86-GT-132, June 8-12, Dusseldorf, Germany, 1986.

[47] G.J. VanFossen, "Heat-transfer coefficients for staggered arrays of short pin fins", Transactions of the ASME, Journal of Heat Transfer. 1982;**104**:268–274.

[48] M.K. Chyu, "Heat transfer and pressure drop for short pin-fin arrays with pin-endwall fillet", ASME Journal of Heat Transfer. 1990;**112**:926–932.

[49] T.K. Kumaran, J.C. Han, and S.C. Lau, "Augmented heat transfer in a pin fin channel with short or long ejection holes", International Journal of Heat Mass Transfer. 1991;**34**;(10):2617–2628.

[50] J. Krueckels, S. Naik, A. Lerch, Heat transfer in a vane trailing edge passage with conical pins and pin-turbulator integrated configurations, Proceedings of ASME Turbo-Expo for Land, Sea and Air, Paper GT2014-25522, June 16-20, Duesseldorf, Germany, 2014.

[51] R. Bunker, Gas turbine heat transfer: 10 remaining hot gas path challenges, GT2006-90002, Proceedings of ASME Turbo Expo 2006: Power for Land, Sea and Air, May 8–11, Barcelona, Spain, 2006.

[52] M.K. Chyu and S.C. Siw, Recent advances of internal cooling techniques for gas turbine airfoils, Journal of Thermal Science and Engineering applications, 2013;**5**:021008-1.

[53] M. Cochet, W. Colban, M. Gritsch, S. Naik, and M. Schnieder, Thermal validation of a heat shield surface for a high lift blade profile, Proceedings of ASME Turbo Expo, Paper GT2011-46294, June 6–10, 2011, Vancouver, Canada, 2011

IntechOpen